Cellular Signalling 25 (2013) 2093–2105

Contents lists available at ScienceDirect

Cellular Signalling

journal homepage: www.elsevier.com/locate/cellsig

Neu1 sialidase and matrix metalloproteinase-9 cross-talk regulates nucleic acid-induced endosomal TOLL-like receptor-7 and -9 activation, cellular signaling and pro-inflammatory responses

Samar Abdulkhalek, Myron R. Szewczuk *

Department of Biomedical & Molecular Sciences, Queen's University, Kingston, Ontario K7L3N6, Canada

ARTICLE INFO

Article history:
Received 22 March 2013
Received in revised form 5 June 2013
Accepted 18 June 2013
Available online 1 July 2013

Keywords:
Neu1 sialidase
GPCR Gα proteins
MMP9
Macrophage cells
TLR signaling
NMBR receptors
GPCR signaling

ABSTRACT

The precise mechanism(s) by which intracellular TOLL-like receptors (TLRs) become activated by their ligands remains unclear. Here, we report a molecular organizational G-protein coupled receptor (GPCR) signaling platform to potentiate a novel mammalian neuraminidase-1 (Neu1) and matrix metalloproteinase-9 (MMP-9) cross-talk in alliance with neuromedin B GPCR, all of which form a tripartite complex with TLR-7 and -9. siRNA silencing Neu1, MMP-9 and neuromedin-B GPCR in RAW-blue macrophage cells significantly reduced TLR7 imiquimod- and TLR9 ODN1826-induced NF-κB (NF-κB-pSer^{536}) activity. Tamiflu, specific MMP-9 inhibitor, neuromedin B receptor specific antagonist BIM23127, and the selective inhibitor of whole heterotrimeric G-protein complex BIM-46174 significantly block nucleic acid-induced TLR-7 and -9 MyD88 recruitment, NF-κB activation and proinflammatory TNFα and MCP-1 cytokine responses. For the first time, Neu1 clearly plays a central role in mediating nucleic acid-induced intracellular TLR activation, and the interactions involving NMBR–MMP9–Neu1 cross-talk constitute a novel intracellular TLR signaling platform that is essential for NF-κB activation and pro-inflammatory responses.

1. Introduction

Dimerization of the extracellular domain of most mammalian TOLL-like receptors (TLRs) is essential for their ligand induced activation. However, the mechanism(s) by which TLRs become activated by this process is not well understood. For the majority of TLR receptors, dimerization is a prerequisite to facilitate MyD88/TLR complex formation and subsequent cellular signaling to activate NF-κB. However, the parameters controlling interactions between the receptors and their ligands remained poorly defined until now. For the cell-surface TLRs, we have identified a novel molecular organizational G-protein coupled receptor (GPCR) signaling platform to potentiate Neu1 sialidase and matrix metalloproteinase-9 (MMP9) cross-talk in regulating endotoxin lipopolysaccharide (LPS) induced TLR4 receptors and cellular function [1–3]. In addition, the activity of these TLRs is also regulated by a variety of other ligand-related cofactors involved in improving ligand recognition by the receptors such as diacylglyceride sensing by CD36 [4,5], CD14 [6], and MD-2 [7,8]. However, there is another subset of TLRs, namely TLR-3, -7, -8, and -9, which are localized within the endosomal compartment of the cell that are known to recognize nucleic acids [9]. Although their subcellular compartmentalization and cellular distribution are maintained in their correct subcellular localization by endoplasmic reticulum (ER) chaperone gp96 [10], protein associated with TLR4 (PRATA/B) [11–13], the ER membrane protein, UNC93B [14,15], and the high-mobility group protein B1 (HMGB1) [16], the mechanistic machinery driving nucleic acid-induced intracellular TLR dimerization and subsequent receptor function is unknown.

To gain an insight into the molecular mechanism of intracellular TLR7 triggering, Visintin and colleagues using N-nitrose-N9-ethyl urea (ENU)-induced mutations in mice identified a crucial role for N-glycosylation target sequence in position 66–68 (N66) within the leucine-rich repeat, LRR1 ectodomain, containing a putative glycan acceptor site, which resulted in the conversion of threonine 68 to isoleucine (T68I) in TLR7 [17]. This TLR7^{rsq1} mutation was found to reside in the N-terminal portion of TLR7, which was found to be in close proximity to the first two insertions thought to be relevant for ligand binding. The abrogation of the N-glycosylation consensus

Abbreviations: TLR, TOLL-like receptors; 4MUNANA, 2′-(4-methylumbelliferyl)-α-D-N-acetylneuraminic acid; Tamiflu, oseltamivir phosphate; MMP, matrix metalloproteinase; GPCR, G-protein coupled receptor; SEAP, secreted embryonic alkaline phosphatase; IC_{50}, 50% inhibitory concentration.

* Corresponding author. Tel.: +1 613 533 2457; fax: +1 613 533 6796.
E-mail addresses: samarma@hotmail.com (S. Abdulkhalek), szewczuk@queensu.ca (M.R. Szewczuk).

0898-6568
http://dx.doi.org/10.1016/j.cellsig.2013.06.010

impaired the ability of TLR7 to signal in response to ssRNA and low molecular weight TLR7 agonist resiquimod (R848), but not its ability to bind to ssRNA. This unexpected ssRNA binding by the mutant TLR7^{rsq1} and lack of signaling implied that the N-glycosylation status of the N-terminal portion of TLR7 is essential for receptor activation and function [17].

In conjunction with the TLR dimerization process, TLR receptors need to undergo conformational changes following ligand binding, which allow proper orientation of the ectodomains of TLR for receptor association [18,19]. Indeed, ligand-induced conformational changes have been shown to allosterically activate TLR9 receptors [20]. Using mutagenesis studies on murine TLR-7 and -9, others have shown sensitivity of these receptors to subtle changes [21]. In another study, we reported the importance of the involvement of α-2,3-sialyl residues linked to β-galactosides in establishing steric hindrance to TLR4 dimerization [22,23]. This novel premise was emphasized by exogenous α-2,3-sialyl specific neuraminidases [23]. Primary bone marrow macrophages derived from Neu1-deficient mice treated with a purified recombinant neuraminidase (*Clostridium perfringens*) or recombinant *Trypanosoma cruzi* trans-sialidase (TS) but not the mutant TSΔAsp98-Glu induced phosphorylation of NF-κB [23]. These results are consistent with our other reports [23–27] supporting the glycosylation model in corroborating the importance of sialyl α-2,3-linked β-galactosyl residues of TLRs as well as for tyrosine receptor kinase Trks in the initial stages of ligand-induced receptor activation. For mammalian sialidases, we have shown that the mammalian neuraminidase-1 (Neu1) desialylation of α-2,3-sialyl residues of cell-surface TLR receptors enables receptor dimerization [23]. Neu1 was found to be an important intermediate in the initial process of TLR ligand-induced receptor activation and subsequent cell function [23,24]. Central to this process is that Neu1, and not the other three mammalian sialidases, forms a complex with either TLR-2, -3 or -4 cell-surface receptors in naive TLR-expressing cells or primary macrophage cells [24]. The prerequisite desialyation of cell-surface TLR receptors caused by activated Neu1 enables MyD88/TLR4 complex recruitment, NFκB activation and pro-inflammatory responses [23,24].

This report describes the key players involved in the activation of nucleic acid sensing intracellular TLR-7 and TLR-9 receptors against imiquimod and CpG oligodeoxynucleotide (ODN), respectively. It discloses a striking identical signaling paradigm as described for the cell-surface TLRs [1–3]. Here, Neu1 and MMP9 cross-talk in alliance with GPCR neuromedin-B receptors tethered to TLR-7 and -9 receptors at the ectodomain forms a novel molecular organizational GPCR signaling platform that is essential for ligand activation of the TLRs and cellular signaling. Since TLR9 receptors are prone to ligand-induced conformational changes in the ectodomains [20], it is proposed here that ligand binding to TLR-7 and -9 receptors initiates a conformational change to potentiate G-protein coupled receptor (GPCR)-signaling via membrane Gα subunit proteins and matrix metalloproteinase-9 (MMP-9) activation to induce Neu1. Activated Neu1 specifically hydrolyzes α-2,3-sialyl residues linked to β-galactosides, the structural perturbation of which would trigger dimeric receptor complex formation to facilitate MyD88/TLR recruitment and subsequent pro-inflammatory cell responses. These findings radically redefine the current dogma(s) governing the essential activating molecules tethered to nucleic acid sensing TLRs, which may provide pioneering molecular targeting approaches to disease intervention strategies.

2. Materials and methods

2.1. Cell lines

The HEK-TLR7-HA cells were obtained by stable transfection of HEK293XL cells with the pUNO-hTLR7-HA plasmid which expresses the human TLR7 gene fused at the 3′ end to the influenza hemagglutinin (HA) (InvivoGen, San Diego, CA). HEK-293 (ATCC® CRL-1573™) were obtained from American Type Culture Collection (Manassas, VA 20110 USA). The cells were grown at 37 °C in 5% CO_2 in culture media containing Dulbecco's Modified Eagle Medium (DMEM) (Gibco, Rockville, MD) supplemented with 10% fetal calf serum (FCS) (HyClone, Logan, Utah, USA) and selection in 100 μg/mL Normocin™. The HEK-293 cells were grown in the same medium without selection antibiotic.

RAW-Blue™ cells (Mouse Macrophage Reporter Cell Line, InvivoGen, San Diego, CA) derived from RAW 264.7 macrophages are grown in culture medium containing Zeocin as the selectable marker. They stably express a secreted embryonic alkaline phosphatase (SEAP) gene inducible by NF-κB and AP-1 transcription factors. Upon stimulation, RAW-Blue™ cells activate NF-κB and/or AP-1 leading to the secretion of SEAP which is detectable and measurable using QUANTI-Blue™, a SEAP detection medium (InvivoGen). RAW-Blue™ cells are resistant to Zeocin™ and G418 in the conditioned medium.

RAW264.7 cells were obtained from Dr Andrew Craig (Queen's University) and maintained in DMEM with 10% FCS and 2 mM L-glutamine at 37 °C in 5% CO_2 humidified incubator.

2.2. Silencing Neu1, MMP-9 and NMBR mRNA using siRNA

Mouse NEU1, MMP9 and NMBR ON-TARGETplus SMART pool, were obtained from Thermo Scientific Dharmacon each containing a mixture of four predesigned siRNAs targeting one gene. RAW-blue cells were plated in 6-well plate at 3×10^5 cells/well and incubated at 37 °C for 24 h or until 50–60% confluent. 250 μL OPTIMEM media (Invitrogen) was pipetted into each of 2 tubes, 100 pmol siRNA was added to one tube and 6 μL Lipofectamine 2000 (Invitrogen) into the other and incubated for 5 min. The Lipofectamine containing tube was transferred into the siRNA containing tube by gently mixing. The mixture was incubated for 20 min at room temperature. During the 20 min incubation, medium was aspirated from the wells containing the cells and replaced with 500 μL of fresh OPTIMEM media and the mixture containing siRNA duplex together with Lipofectamine 2000 complexes was added to each well incubating for 5–6 h at 37 °C in a humidified 5% CO_2 incubator. At the end of transfection, the mixture is replaced with fresh complete media and plate is incubated for 24 h. The process of siRNA transfection was repeated on these same transfected cells. The transfection efficiency of 90% was determined using fluorescein conjugated control siRNAs (Santa Cruz Biotech) and counting the proportion of labeled cells using fluorescence microscopy (Zeiss Imager M2). 72 h post double siRNA transfection, RAW-blue cells were assayed for protein level to assess silencing.

2.3. Ligands

TLR7 ligand, Imiquimod from BioVision was used at 10 or 20 μg/mL. TLR9 ligand, ODN 1826 from InvivoGen was used at 10 or 20 μg/mL. ODN 1826 is a type B CpG ODN specific for mouse TLR9. Type B CpG ODNs contain a full phosphorothioate backbone with one or more CpG dinucleotides. They strongly activate B cells but weakly stimulate IFN-α secretion.

2.4. Inhibitors

Tamiflu (pure oseltamivir phosphate, Hoffmann-La Roche Ltd., Mississauga, Ontario, Lot # S00060168) was used at indicated concentrations. MMP-3 inhibitor (MMP3i; stromelysin-1 inhibitor, Calbiochem-EMD Chemicals Inc.) inhibits MMP-3 (IC_{50} = 5 nM). MMP-9 inhibitor (MMP9i, Calbiochem-EMD Chemicals Inc.) is a cell-permeable, potent, selective, and reversible MMP-9 inhibitor (IC_{50} = 5 nM). It inhibits MMP-1 (IC_{50} = 1.05 μM) and MMP-13

(IC_{50} = 113 nM) only at much higher concentrations. BIM-46174 is a G-protein inhibitor kindly provided by IPSEN Innovation (91940 Les Ulis, France). BIM-23127 is a specific neuromedin B receptor inhibitor from Tocris Bioscience (Tocris House, IO Centre Moorend Farm Avenue, Bristol, BS11 0QL, United Kingdom).

2.5. NF-κB-dependent secretory alkaline phosphatase (SEAP) assay

Briefly, a cell suspension of 1×10^6 cells/mL in fresh growth medium was prepared, and 100 μL of cell suspension (~100,000 cells) was added to each well of a Falcon flat-bottom 96-well plate (Becton Dickinson). Different concentrations of either specific MMP9 inhibitor (MMP9i) common Tamiflu or BIM-46174 were added to each well 1 h before ligand stimulation. The plates were incubated at 37 °C in a 5% CO_2 incubator for 18–24 h. A QUANTI-Blue™ (InvivoGen) solution which is a detection medium developed to determine the activity of any alkaline phosphatase present in a biological sample was prepared following the manufacturer's instructions. Briefly, 160 μL of resuspended QUANTI-Blue solution was added to each well of a flat-bottom 96-well plate, followed by 40 μL of supernatant from stimulated RAW-blue cells. The plate was incubated for 60 min at 37 °C and the SEAP levels were determined using a spectrophotometer at 620–655 nm. Each experiment was performed in triplicates.

2.6. Co-immunoprecipitation

Macrophage cells were left cultured in media or in media containing 20 μg/mL imiquimod or ODN for indicated time intervals. Cells (1×10^7 cells) are pelleted and lysed in lysis buffer (50 mM Tris, pH 8, 150 mM NaCl, 1% NP-40, 0.2 mg/mL) containing Halt Protease and Phosphatase Inhibitor cocktail (Thermo Scientific). For immunoprecipitation, Neu1, MMP-9, TLR7, TLR9 or NMBR in cell lysates from RAW-blue cells are immunoprecipitated with 1.0 μg of either rabbit anti-Neu1, rabbit anti-MMP-9, rabbit anti-TLR7, rabbit anti TLR9 or rabbit anti-NMBR antibodies for 24 h. Following immunoprecipitation, complexes are isolated using protein A or G magnetic beads, washed 3× in buffer (10 mM Tris, pH 8, 1 mM EDTA, 1 mM EGTA, 150 mM NaCl, 1% Triton X-100 and 0.2 mM sodium orthovanadate) and resolved by 8% gel electrophoresis (SDS-PAGE). Proteins are transferred to polyvinylidene fluoride (PVDF) transfer membrane blot. The blots are probed for either MMP-9 with anti-MMP-9 (H-129, Santa Cruz Biotechnology, Inc. CA), Neu1 with anti-Neu1 (H-300, Santa Cruz Biotech), TLR7 with anti-TLR7 (H-114, Santa Cruz Biotech), TLR9 with anti TLR9 (H-100, Santa Cruz Biotechnology) or NMBR with anti-NMBR (M-52, Santa Cruz Biotechnology) followed by HRP conjugated secondary IgG antibodies or Clean-Blot IP Detection Reagent for IP/Western blots (Pierce Biotechnology, Thermo Fisher Scientific, Rockford, IL) and Western Lightning Chemiluminescence Reagent Plus. The chemiluminescence reaction was analyzed with X-ray film. Sample concentration for gel loading was determined by the Bradford reagent (Sigma-Aldrich Canada Ltd., Oakville, Ontario).

2.7. Neu1 or MMP9 colocalization with TLR-7 and -9

RAW-blue macrophage cells were cultured in DMEM medium with 10% FCS. Cells were treated with 20 μg/mL imiquimod or 20 μg/mL ODN for 30 min or left untreated as controls. Cells were fixed, permeabilized and immunostained with either rabbit anti-TLR7 (H-114, Santa Cruz Biotech) or rabbit anti-TLR9 (H-100, Santa Cruz Biotech) and goat anti-MMP-9 (M-17, Santa Cruz Biotechnology) or goat anti-Neu1 (N-20, Santa Cruz Biotechnology) followed with Alexa Fluor488 donkey anti-rabbit IgG or Alexa Fluor594 donkey anti-goat IgG. Stained cells were visualized using a Zeiss M2 Imager with a 40× objective. Images were processed using Image J 1.38x software (NIH, USA). To calculate the amount of colocalization in the selected images, the Pearson correlation coefficient was measured and expressed as a percentage using Image J 1.38x software.

2.8. GPCR neuromedin-B receptor (NMBR) colocalization with Rab7

RAW-blue mouse macrophage cells were cultured in DMEM medium with 10% FCS. Cells were fixed, permeabilized and immunostained with rabbit anti-NMBR (M-52, Santa Cruz Biotechnology, Inc., California, USA) and mouse monoclonal anti-Rab7 (Abcam) followed with Alexa Fluor568 donkey anti-mouse IgG or Alexa Fluor488 donkey anti-rabbit IgG. Stained cells were visualized using a Zeiss M2 Imager with a 40× objective. Images were captured and processed using Image J 1.38x software (NIH, USA). To calculate the amount of colocalization in the selected images, the Pearson correlation coefficient was measured and expressed as a percentage using Image J 1.38x software.

2.9. Bio-Plex cytokine microarray profiles in the cell culture supernatants using the multiplex bead-based assay

RAW-blue mouse macrophage cells were grown at 3×10^4 cells/well in flat-bottom 96-well plate at 37 °C and 5% CO_2 for 18–24 h. Media was discarded and 100 μL of fresh media alone or with inhibitors at indicated concentrations was added to the wells, and the plate was incubated for 60 min before adding the specific ligand. The plate was incubated for an additional 24 h. Supernatants were collected and the assay was carried out according to the manufacturer's instructions. The cytokines in individual supernatant samples were measured using the Bio-Plex 200 System and quantified using standard curve for each cytokine.

2.10. Statistics

Comparisons between two groups were made by one-way ANOVA at 95% confidence using unpaired t-test and Bonferroni's Multiple Comparison Test or Dunnett's Multiple Comparison Test for comparisons among more than two groups.

3. Results

3.1. Neu1 and MMP-9 cross-talk is tethered to naive full-length and cleaved TLR7 receptors

According to the trafficking and processing models of intracellular TLRs [9], TLR3, TLR7, TLR8, TLR9, and probably TLR13 of mice, are expressed within the endoplasmic reticulum (ER), endosomes, multi-vesicular bodies, and lysosomes. However, ligand-induced TLR activation only occurs within acidified endolysosomal compartments. Upon reaching these acidified compartments, the TLR9 ectodomain is proteolytically cleaved by proteases [28,29]. However, the full-length TLR9 is found only in the ER, whereas the cleaved, biologically active product is restricted to endolysosomes. Multiple proteases have been implicated in TLR9 cleavage, including various cathepsins and asparagine endopeptidase [28–33] as well as asparagine endopeptidase cleavage of TLR7 [34].

For cell-surface TLR4 receptors, we reported a receptor signaling paradigm involving a process of receptor ligand-induced GPCR-signaling via Gαi-proteins, MMP-9 activation, and the induction of Neu1 activation [2]. To test whether this signaling paradigm is involved with full-length and cleaved intracellular TLRs, we initially asked whether Neu1 and MMP9 form a complex with TLR7 receptors. Co-immunoprecipitation experiments using cell lysates from HEK-TLR7-HA cells demonstrated that both Neu1 and MMP-9 are tethered to full-length (120 kDa) and cleaved (72 kDa) TLR7 receptors in naive and 30 min imiquimod stimulated cells (Fig. 1A and B). However, only Neu1 and Neu4 but not Neu-2 and -3 co-immunoprecipitated

with full-length 120 kDa TLR7 in the cell lysates of HEK-TLR7-HA cells (Fig. 1B). Recent reports by us have indicated that Neu4 is tethered to MMP9 but requires a special ligand to become activated [35,36]. In support of the co-immunoprecipitation results with HEK-TLR7-HA cells, the data shown in Fig. 1C–D validated the predicted association of Neu1 and MMP9 with TLR7. Zeiss M2 Imager fluorescence microscopy revealed the endosomal colocalization of Neu1 and MMP9 with TLR7 in naive and imiquimod-treated RAW-blue cells. There was no marked reduction of Neu1 (30.8% overlay) and MMP9 (47.0% overlay) colocalization with TLR7 in these cells treated with imiquimod for 60 min compared with the untreated control cells (33.4% overlay for Neu1 and 40.9% for MMP9). As predicted, Neu1 and the active 65 kDa isoform of MMP9 also co-immunoprecipitated with TLR7 in cell lysates from naive and imiquimod-treated RAW-blue cells with no diminution of Neu1 and MMP9 after 15–60 min (Fig. 1E). Conversely, the cleaved 72 kDa and possibly 65 kDa TLR7 co-immunoprecipitated with both Neu1 and MMP9 in cell lysates from naive and 30 min imiquimod-treated RAW-blue cells (Fig. 1F).

3.2. TLR7 and TLR9 signaling is independent of TLR4

A recent report has demonstrated that ODN stimulation of human lung cancer cells induced the secretion of high-mobility group protein B1 (HMGB1) dose-dependently [37]. The cell response to HMGB1 stimulation acting synergistic with ODN mediated a MyD88-dependent up-regulation of MMP2, MMP9 and cyclin-dependent

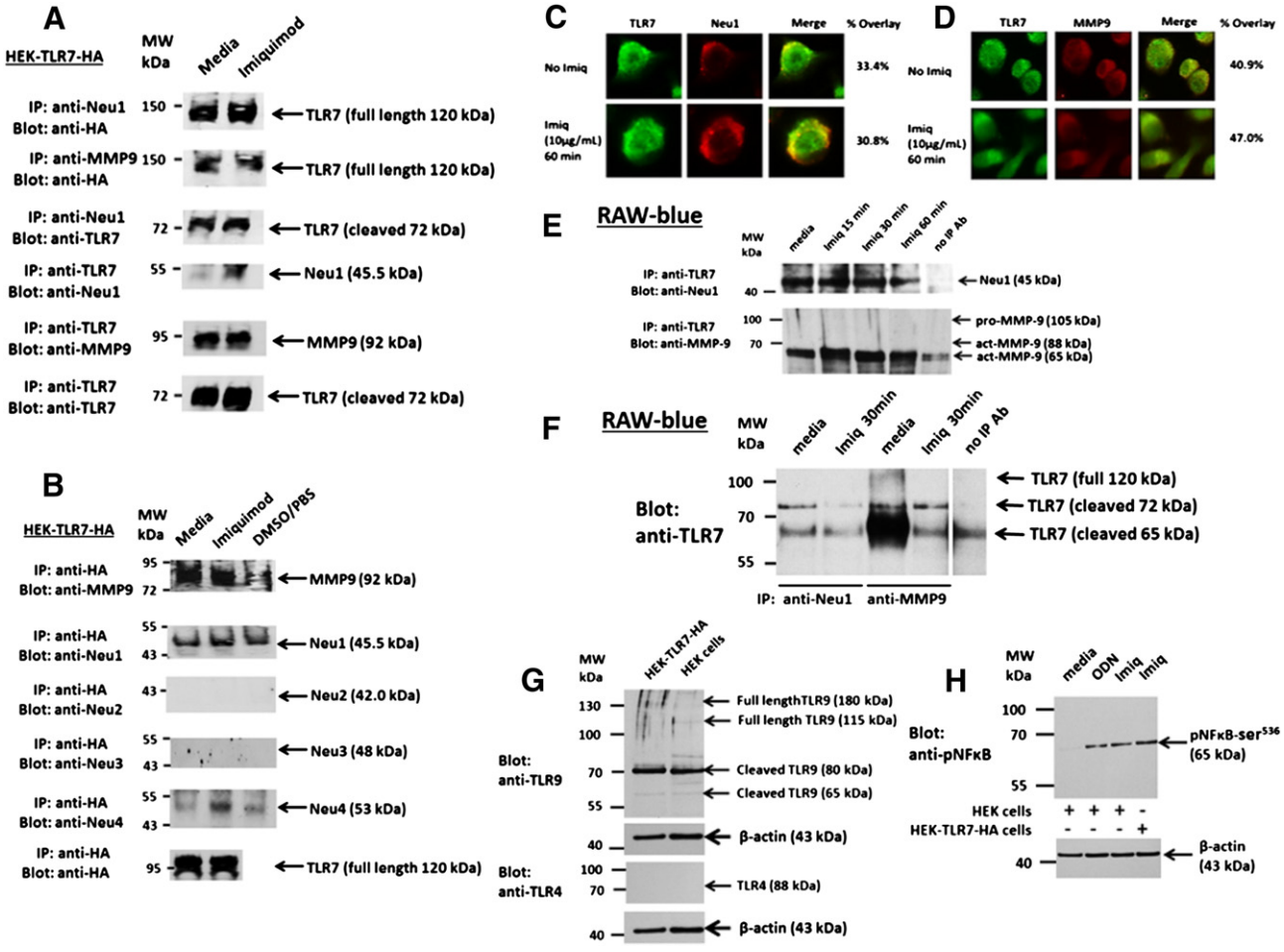

Fig. 1. TLR7 co-immunoprecipitates with Neu1 and MMP9 and conversely vice-versa. HEK-TLR7-HA (A) and RAW-blue (E and F) cells were left cultured in media or in media containing 10 μg/mL imiquimod for 30 min or indicated times. Cells (1×10^7 cells) were pelleted and lysed in lysis buffer. Neu1, MMP9, TLR7-HA and TLR7 receptors in the cell lysates from either HEK-TLR7-HA or RAW-blue cells were immunoprecipitated with 1 μg of rabbit anti-Neu1, rabbit anti-MMP9 or 1 μg of rabbit anti-HA antibodies for 24 h. Following immunoprecipitation, complexes were isolated using protein A or G magnetic beads, washed 3× in buffer and resolved by 8% SDS-PAGE. The blots were probed for HA with anti-HA or TLR7 with anti-TLR7 antibodies followed by Clean-Blot IP Detection Reagent for IP/Western blots and Western Lightning Chemiluminescence Reagent Plus. The chemiluminescence reaction was analyzed with X-ray film. Sample concentration for gel loading was determined by Bradford assay. The data are a representation of one out of three independent experiments showing similar results. (B) Neu1 co-immunoprecipitates withTLR7. HEK-TLR7-HA cells were used as described in (A). They were pelleted, lysed in lysis buffer and the protein lysates were resolved by SDS-PAGE. The blots were probed with antibodies against the indicated proteins. DMSO/PBS: cells were treated with DMSO in PBS before lysing to control for the effect of imiquimod reagent diluent. (C) Neu1 and MMP9 colocalize with TLR7. RAW-blue cells (50,000 cells) were plated on 12 mm circular glass slides in culture media containing 10% fetal calf sera for 24 h and treated with 10 μg/mL imiquimod for 60 min or left untreated as controls. Cells were fixed, permeabilized and immunostained with rabbit anti-TLR7 and goat anti-Neu1 or goat anti-MMP9 followed with Alexa Fluor488 donkey anti-rabbit IgG or Alexa Fluor594 donkey anti-goat IgG. Stained cells were visualized using a Zeiss M2 imager with a 40× objective. To calculate the percentage of colocalization in the selected images, the Pearson correlation coefficient was measured on a total of 15–20 cells per image and expressed as a percentage using Image J 1.38x software. The data are a representation of one of three independent experiments showing similar results. (G) Western blot of TLR-4 and -9 expressions in the cell lysates of HEK-293 and HEK-TLR7-HA cells. Unstimulated cells (1×10^7 cells) were pelleted and lysed in lysis buffer. The TLR9 and TLR4 receptors in the cell lysates were separated by SDS-PAGE, and the blot was probed with anti-TLR9 or anti-TLR4 antibodies. β-Actin was used as an internal control protein for loading of the cell lysate. The data are a representation of one of two independent experiments showing similar results. (H) Western blot analysis of ODN- and imiquimod-induced phosphorylated NF-κB (Ser(P)^{536}) in cytoplasmic cell lysates. HEK-293 and HEK-TLR7-HA cells were stimulated with either 10 μg/mL imiquimod or 10 μg/mL ODN for 30 min or left untreated as media control. Cells (1×10^7 cells) were pelleted and lysed in lysis buffer. Cell lysates were separated by SDS-PAGE, and the blot was probed with phospho-specific polyclonal rabbit antibody against NF-κB (Ser(P)^{536}) with minimal reactivity with non-phosphorylated p65. β-Actin was used as an internal control protein for loading of the cytoplasmic cell lysate. The data are a representation of one of two independent experiments showing similar results.

kinase-2 (CDK2), which was critically dependent on the 35 kDa RAGE, the receptor for advanced glycation endproducts and TLR4 [37]. If ODN-induces HMGB1 secretion in these cancer cells, we asked whether HMGB1 might have a role in the ODN-induced NFκB activation via a TLR4 intermediary in our studies. To test this important question, we initially performed Western blot analyses of HEK-TLR7-HA and HEK-293 cells for TLR4 and TLR9 expressions in the cell lysates followed with NFκB activation associated with ODN- and imiquimod-treated cells. Optimal activation of NF-κB requires phosphorylation in the transactivation domain of p65. This transactivation domain of p65 subunit is responsible for the interaction with the inhibitor IκB and contains the phosphorylation sites. A phospho-specific polyclonal antibody against the human NF-κB pSer^{536} that has minimal reactivity with non-phosphorylated p65 was used here. The data shown in Fig. 1G clearly indicate that HEK-293 and HEK-TLR7-HA cells express TLR9 but not TLR4 receptors. In Fig. 1H, the data indicate that ODN and imiquimod induce the 65 kDa NFκB pSer^{539} phosphorylation in these cells, which did not involve the TLR4 as an intermediary. These results are consistent with another reported finding [38].

3.3. Inhibitory effect of Tamiflu, MMP9 inhibitor, a neuromedin B receptor specific antagonist BIM23127, and a selective inhibitor of whole heterotrimeric G-protein complex BIM46174 on imiquimod-induced phosphorylation of NF-κB

To gain insight into the mechanism of action of these nucleic acid sensing receptors, we used RAW-blue cells and asked whether inhibitors of Neu1 and MMP9 would block MyD88 recruitment, phosphorylation of NF-κB and subsequent SEAP secretion associated with imiquimod- or ODN-treated cells. The data shown in Fig. 2C indicate a differential optimal activation of NF-κB associated with imiquimod and ODN treated RAW-blue cells. Cells treated with imiquimod induced optimal NF-κB pSer^{536} activity after 30 min followed by a concomitant decline at 45 and 60 min. However, ODN induced NF-κB pSer^{536} activity after 45 min with a marked decline after 60 min of treatment.

The inhibitory effect of Tamiflu, MMP9 inhibitor (MMP9i), a neuromedin B GPCR specific antagonist BIM23127, and a selective inhibitor of the whole heterotrimeric G-protein complex named BIM-46174 [39], an imidazo-pyrazine derivative, on imiquimod-induced NFκB phosphorylation was also examined in RAW-blue macrophage cells. The data shown in Fig. 2D show that these specific compounds inhibited imiquimod-induced NF-κB pSer^{536} activation in these cells comparable to the no ligand control levels and compared with the imiquimod positive control.

3.4. Interference Neu1, MMP-9 and neuromedin B (NMBR) using siRNA knockdown

To further confirm the role of Neu1, MMP9 and heterotrimeric G-protein NMBR complex in imiquimod-induced NF-κB pSer^{536} activation, we transfected RAW-blue cells with either siRNA Neu1, siRNA MMP9 or siRNA NMBR using ON-TARGETplus SMART pool, each containing a mixture of four predesigned siRNAs targeting one gene using OPTIMEM media and Lipofectamine 2000 reagent. Previously, we reported that when using this transfection protocol, Western blot analyses of whole cell lysates from siRNA MMP9 KD RAW-blue cells revealed a complete knockdown of the active 88 kDa isoform of MMP9 compared to the wild-type (WT) control, but there appeared to be a pro-active MMP-9 (105 kDa) protein fragment that was still present [2]. Western blot analyses of the WT and siRNA Neu1 KD, MMP9 KD and NMBR KD in RAW-blue cells revealed a complete reduction of 65 kDa NF-κB pSer^{536} protein levels in the cell lysates from imiquimod-treated siRNA KD cells compared to the WT controls and β-actin (Fig. 2D). Scrambled siRNA had no effect on 30 min imiquimod-induced NF-κB pSer^{536} levels using the parental RAW264.7 cells (Fig. 2E). Western blot analyses of whole cell lysates from siRNA NMBR KD (Fig. 2F) and siRNA Neu1 KD (Fig. 2G) RAW-blue cells revealed a marked knockdown of the three isoforms of NMBR as well as Neu1 compared to the WT and scrambled siRNA controls. For siRNA MMP9 KD, we reported using western blot analyses of whole cell lysates that siRNA MMP9 KD RAW-blue cells revealed a complete knockdown of the active 88-kDa isoform of MMP9 compared with the WT results, but there appeared to be a proactive 105 kDa MMP9 isoform present [2].

3.5. Tamiflu, MMP9i and neuromedin B GPCR antagonist BIM-23127 inhibit imiquimod-induced TLR7 recruitment of adaptor molecule MyD88 in RAW-blue cells

Since Tamiflu, MMP9i and GPCR antagonist BIM23127 inhibit imiquimod-induced NF-κB pSer^{536} activation in RAW-blue cells (Fig. 2D), we further assessed if they would inhibit imiquimod-mediated recruitment of the adaptor molecule MyD88 to TLR7. Our data clearly show this to be the case. MyD88 co-immunoprecipitated with the 65 kDa cleaved TLR7 receptor following stimulation with imiquimod for 30 min, and this co-IP effect was blocked by Tamiflu, MMP9i and BIM23127 (Fig. 3A). It is well known that both TLR-7 and -9 are completely dependent upon MyD88 in eliciting a signal [9], and our data are consistent with this model. However, the process(es) by which nucleic acid sensing TLRs undergo ligand-induced conformational changes to make them competent to signal is not well understood. For an efficient TLR7 signaling, cleavage of the TLR7 receptor is required for ligand binding and subsequent association with MyD88. Our data here provide evidence for another level of ligand-induced TLR activation. They support an unprecedented unique organizational GPCR signaling platform tethered to TLR7 receptors as the initial processing stage for imiquimod-induced activation of these receptors and subsequent recruitment of the adaptor molecule MyD88.

To confirm Neu1 and MMP9 linkage with imiquimod-induced NFκB activation, we also performed the NFκB-dependent secretory alkaline phosphatase (SEAP) assay. RAW-blue cells stably express a *SEAP* gene inducible by NF-κB and AP-1 transcription factors leading to the secretion of SEAP. Secreted SEAP is detectable and measurable using QUANTI-Blue substrate. Here, we used Tamiflu, MMP9i, the specific inhibitor of MMP3 (MMP3i) and BIM-46174 antagonist of the whole heterotrimeric G-protein complex to determine their inhibitory effects on imiquimod-induced NF-κB activation and subsequent SEAP activity in live RAW-blue cells. The NFκB-dependent SEAP assay shown here clearly demonstrated that BIM-46174 (IC_{50} = 7.94 μM) (Fig. 3B), MMP9i (IC_{50} = 100 μM) and Tamiflu (IC_{50} = 240 μM) (Fig. 3C) dose-dependently attenuated SEAP activity compared with a lack of inhibition with MMP3i (IC_{50} > 1000 μM) (Fig. 3B) associated with imiquimod-treated live RAW-blue cells.

3.6. Neu1 and MMP-9 cross-talk is essential for TLR9 receptor activation and cellular signaling

If Neu1 and MMP-9 complex is tethered to TLR7 receptors, we asked whether they would also colocalize with TLR9 receptors. Fluorescence microscopy revealed the intracellular colocalization of Neu1 and MMP-9 with TLR9 in naive and ODN-treated RAW-blue cells (Fig. 4A and B). Surprisingly, ODN treatment of these cells did not increase the colocalization of TLR9 and MMP-9 (Fig. 4B). Co-immunoprecipitation experiments using cell lysates from RAW-blue cells further demonstrated that Neu1 forms a complex with TLR9 receptors in naive and ODN treatment of cells for 30 min (Fig. 4C). In addition, the two active isoforms of MMP9 (65 and 88 kDa) were found to co-immunoprecipitate with TLR9 in the cell lysates of naive and 30 min ODN-treated RAW-blue cells (Fig. 4C), and conversely, the cleaved

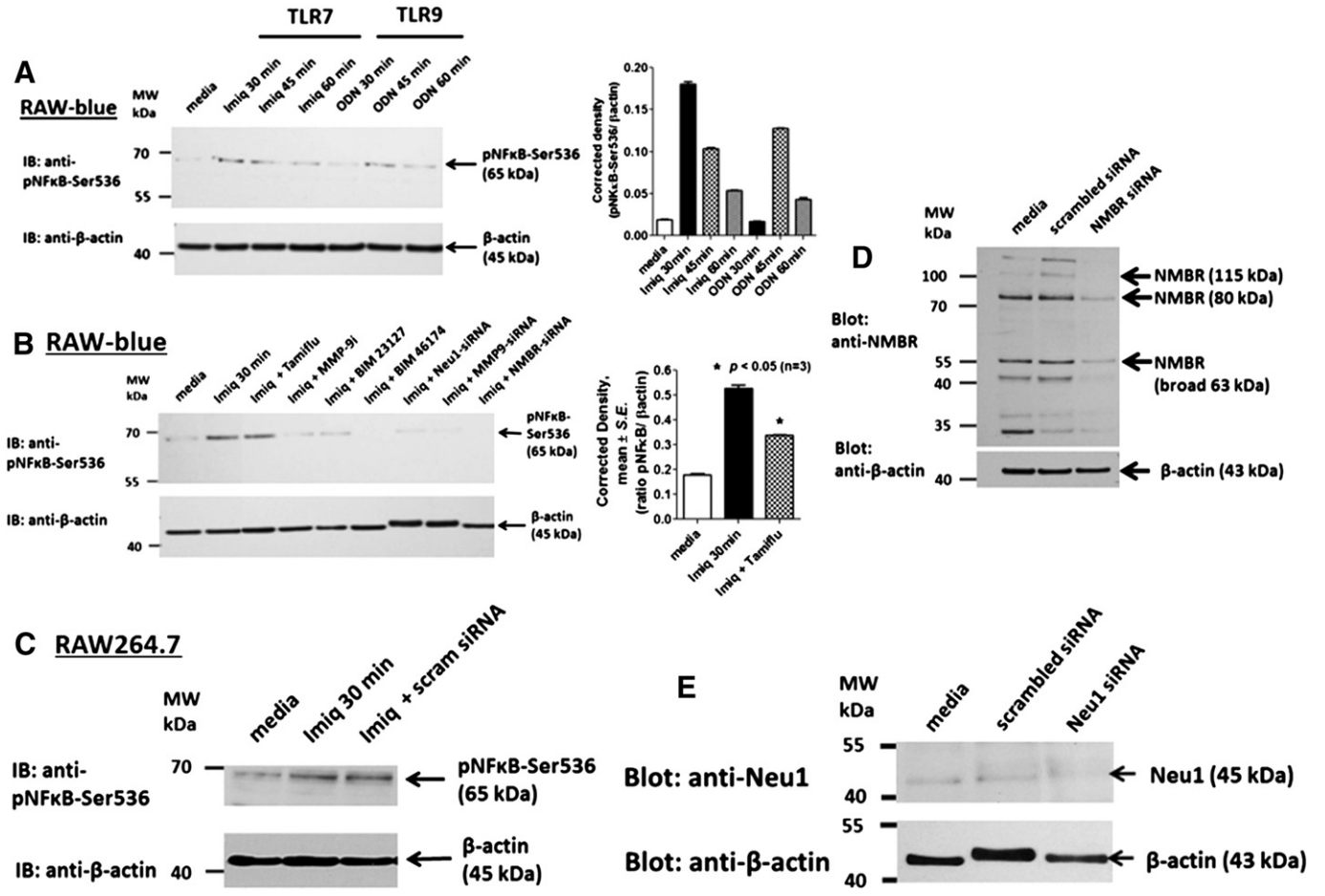

Fig. 2. (A) Western blot analysis of imiquimod- and ODN-induced phosphorylated NF-κB (Ser(P)^{536}) in cytoplasmic cell lysates. RAW-blue cells were treated with either 10 μg/mL imiquimod or 10 μg/mL ODN for the indicated times or left untreated as media control. Cells (1×10^7 cells) were pelleted and lysed in lysis buffer. Cell lysates were separated by SDS-PAGE, and the blot was probed with phospho-specific polyclonal rabbit antibody against NF-κB (Ser(P)^{536}). β-Actin was used as an internal control protein for loading of the cytoplasmic cell lysate. Quantitative analysis was done by assessing the density of a band corrected for background in each lane using Corel Photo Paint 8.0 software. Each bar in the graphs represents the mean ratio of NF-κB (Ser(P)^{536}) to β-actin of band density ± *S.E.* (error bars) for 5–10 replicate measurements. The data are a representation of one of three independent experiments showing similar results. (C) Western blot analysis of imiquimod-induced phosphorylated NF-κB (Ser(P)^{536}) in cytoplasmic cell lysates from wild-type (WT) and siRNA knockdown (KD) cells. RAW-blue macrophage cells were pretreated with 200 μM Tamiflu, 100 μg/mL MMP9i, 100 μg/mL BIM-23127 or 20 μM BIM-46174 for 30 min followed by 10 μg/mL imiquimod. RAW-blue siRNA KD Neu1, siRNA KD MMP9 and siRNA KD NMBR cells were treated with 10 μg/mL imiquimod. Cell lysates from the WT and KD cells were separated by SDS-PAGE, and the blot was probed with phospho-specific polyclonal rabbit antibody against NF-κBp65-Ser(P)^{536}. (D) RAW-blue cells were transfected with scrambled siRNA and stimulated with10 μg/mL imiquimod. β-Actin was used as internal control proteins for loading of the cell lysate and scrambled siRNA transfected cells for transfection control. The data in (C) and (D) are a representation of one of three independent experiments showing similar results. Western blot of NMBR (D) and Neu1 (E) expressions in the cell lysates of unstimulated, scrambled siRNA, NMBR siRNA KD and Neu1 siRNA KD RAW-blue cells. Cells (1×10^7 cells) were pelleted and lysed in lysis buffer. The NMBR and Neu1 proteins in the cell lysates were separated by SDS-PAGE, and the blot was probed with anti-NMBR or anti-Neu1 antibodies. β-Actin was used as an internal control protein for loading of the cell lysate. The data are a representation of one of two independent experiments showing similar results.

65 kDa and 80 kDa isoforms of TLR9 co-immunoprecipitated with both Neu1 and MMP9 in the same cell lysates (Fig. 4D).

At the genetic level, Western blot analyses of the WT and siRNA Neu1 KD, MMP9 KD and NMBR KD in RAW264.7 cells revealed a significant reduction of 65 kDa NF-κB pSer^{536} protein levels in the cell lysates associated with ODN-treated cells compared to the WT controls and β-actin (Fig. 4E). Scrambled siRNA had no significant effect on ODN-induced NF-κB pSer^{536} levels (Fig. 4E). Collectively, the additional intracellular co-localization of TLR9 and Neu1-MMP-9 complex validated the predicted alliance between TLR9 and Neu1-MMP-9.

If Neu1 and MMP9 form a complex with TLR9, inhibitors against these enzymes should block ODN-induced phosphorylation of NFκB in RAW-blue cells. Cells treated with MMP9i and Tamiflu inhibited ODN-induced pNFκB in the cell lysates compared to the ODN-treated positive control and the β-actin (Fig. 5A). Live cells pretreated with MMP3i or anti-Neu1 antibody followed with ODN stimulation showed no reduction of pNF-κB activity in the cell lysates. As expected, the anti-Neu1 antibody treatment of the live cells would not be internalized into the endosomal compartment to neutralize Neu1 activity (Fig. 5A).

To confirm Neu1 and MMP9 linkage with ODN-induced NFκB activation, we also performed the SEAP assay as well. We used MMP3i, MMP9i, Tamiflu and BIM-46174 to determine their inhibitory effects on ODN-induced SEAP activity in live RAW-blue cells. The data shown in Fig. 5B–C clearly demonstrate that MMP9i (IC_{50} = 199 μM) (Fig. 5B), Tamiflu (IC_{50} = 398 μM) (Fig. 5B) and BIM-46174 (IC_{50} = 20 μM) (Fig. 5C), but not MMP3i (IC_{50} > 1000 μM) (Fig. 5C) dose-dependently blocked the NFκB-dependent SEAP activity associated with ODN treated live RAW-blue cells.

3.7. Isoforms of neuromedin B GPCR co-immunoprecipitate with TLR-7 and -9 receptors in cell lysates from naive and ligand stimulated RAW-blue cells

Since neuromedin B receptor antagonist BIM-23127 and the heterotrimeric G-protein complex antagonist BIM-46174 block

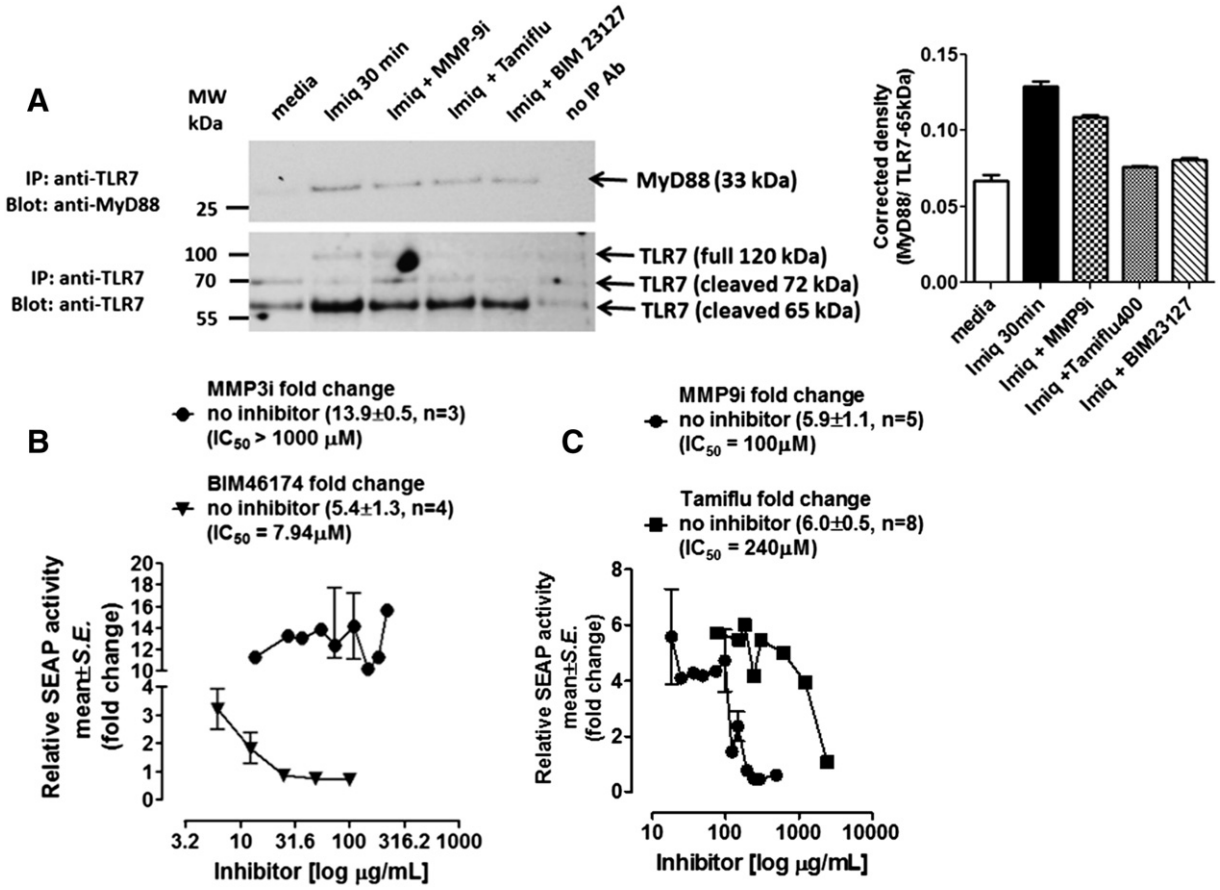

Fig. 3. (A) MyD88 co-immunoprecipitates with TLR7. RAW-blue cells were pretreated with 200 μM Tamiflu, 100 μg/mL MMP9i, or 100 μg/mL BIM-23127 for 30 min followed by 10 μg/mL imiquimod or left cultured in media. Cells (1×10^7 cells) are pelleted and lysed in lysis buffer. TLR7 in cell lysates is immunoprecipitated with 1.0 μg of rabbit anti-TLR7 antibodies for 24 h. Following immunoprecipitation, complexes are isolated using protein A or G magnetic beads, washed 3× in buffer and resolved by 8% SDS-PAGE. The blots are probed for MyD88 (33 kDa) with anti-MyD88 antibodies followed by Clean-Blot IP Detection Reagent for IP/Western blots and Western Lightning Chemiluminescence Reagent Plus. The chemiluminescence reaction was analyzed with X-ray film. Sample concentration for gel loading was determined by Bradford assay. The data are a representation of one of three independent experiments showing similar results. (B and C) BIM-46174, Tamiflu and MMP9i but not MMP3i inhibit dose-dependently NF-κB-dependent SEAP activity associated with imiquimod-treated SEAP reporter-expressing RAW-blue cells. Cells (1×10^5 cells) were treated with different doses of MMP3i inhibitor, MMP9i, Tamiflu and BIM46174 for 24 h. The SEAP activity in the culture medium was assessed using QUANTI-Blue substrate. Relative SEAP activity was calculated as fold change of each compound (SEAP activity in medium from treated cells minus no cell background over SEAP activity in medium from untreated cells minus background). The SEAP activity in the absence of inhibitors is indicated. The 50% inhibition concentration (IC_{50}) for each inhibitor on SEAP activity induced by imiquimod was determined by plotting the decrease in SEAP activity against the log of the agent concentration. The data are a representation of mean ± *S.E.* (n = 3–8 independent experiments as indicated).

NF-κB activation associated with imiquimod- and ODN-stimulated RAW-blue cells (Figs. 2D, 3B and 5C) and MyD88 recruitment associated with imiquimod-stimulated cells (Fig. 3A), we questioned whether the bombesin-like receptor, neuromedin B (NMBR) forms a complex with TLR-7 and -9 receptors. Co-immunoprecipitation experiments using cell lysates from RAW-blue cells showed that the broad range 63 kDa isoform of NMBR forms a complex tethered to the cleaved 65 kDa and full length 180 kDa TLR-9 (Fig. 6A) and cleaved 65 kDa TLR-7 (Fig. 6B) in naive and 60 min ligand-treated cells. In addition, the 80 kDa isoform of NMBR co-immunoprecipitated with MMP9, and conversely, the 88 kDa isoform of MMP9 co-immunoprecipitated with NMBR in the same cell lysates (Fig. 6C). Indeed, it is well known that agonist-bound GPCRs have been shown to activate numerous MMPs [40], including MMP9 [41,42]. However, the precise molecular mechanism(s) underlying GPCR-mediated MMP activation is unclear. Perhaps, it might involve a conformational change following TLR ligand binding. It has been reported that the binding of ODN to TLR9 receptors leads to substantial conformational changes in the TLR9 ectodomain [20,28,43]. The data in Fig. 6A and B indicate a direct linkage between NMBR and MMP9 at the ectodomains of TLR-7 and -9 receptors. These interesting findings are strikingly consistent with our other report showing a direct linkage between NMBR and MMP9 at the ectodomain of TLR4 on the cell surface [3].

To confirm these findings, we used BIM-23127 and BIM-46174 to test their inhibitory effects on SEAP activity associated with ODN and imiquimod treated RAW-blue cells. As expected, BIM-23127 and BIM-46174 significantly inhibited SEAP activity associated with ODN (Fig. 6D) and imiquimod (Fig. 6E) stimulation of live SEAP-reporter RAW-blue cells. The NFκB-dependent SEAP assay shown in Fig. 6F demonstrates that siRNA NMBR KD in RAW-blue cells significantly inhibited SEAP activity compared to the WT cells associated with imiquimod stimulated live cells. Collectively, the data validated the predicted alliance between nucleic acid sensing TLR-7 and -9 receptors and NMBR in naive macrophage cells. They also support recent evidence for a novel concept of intracellular GPCR signaling where it suggests new and intriguing scenarios for the functions of GPCRs in the endocytic compartments [44,45]. To confirm the location of neuromedin B receptor (NMBR) in the endocytic compartment, we asked whether the small GTP binding protein Rab7 which has a role in the late endocytic pathway and lysosome biogenesis would colocalize with NMBR receptors. The data in Fig. 6G show this to be the case. NMBR colocalizes with Rab7 associated with naive RAW-blue cells.

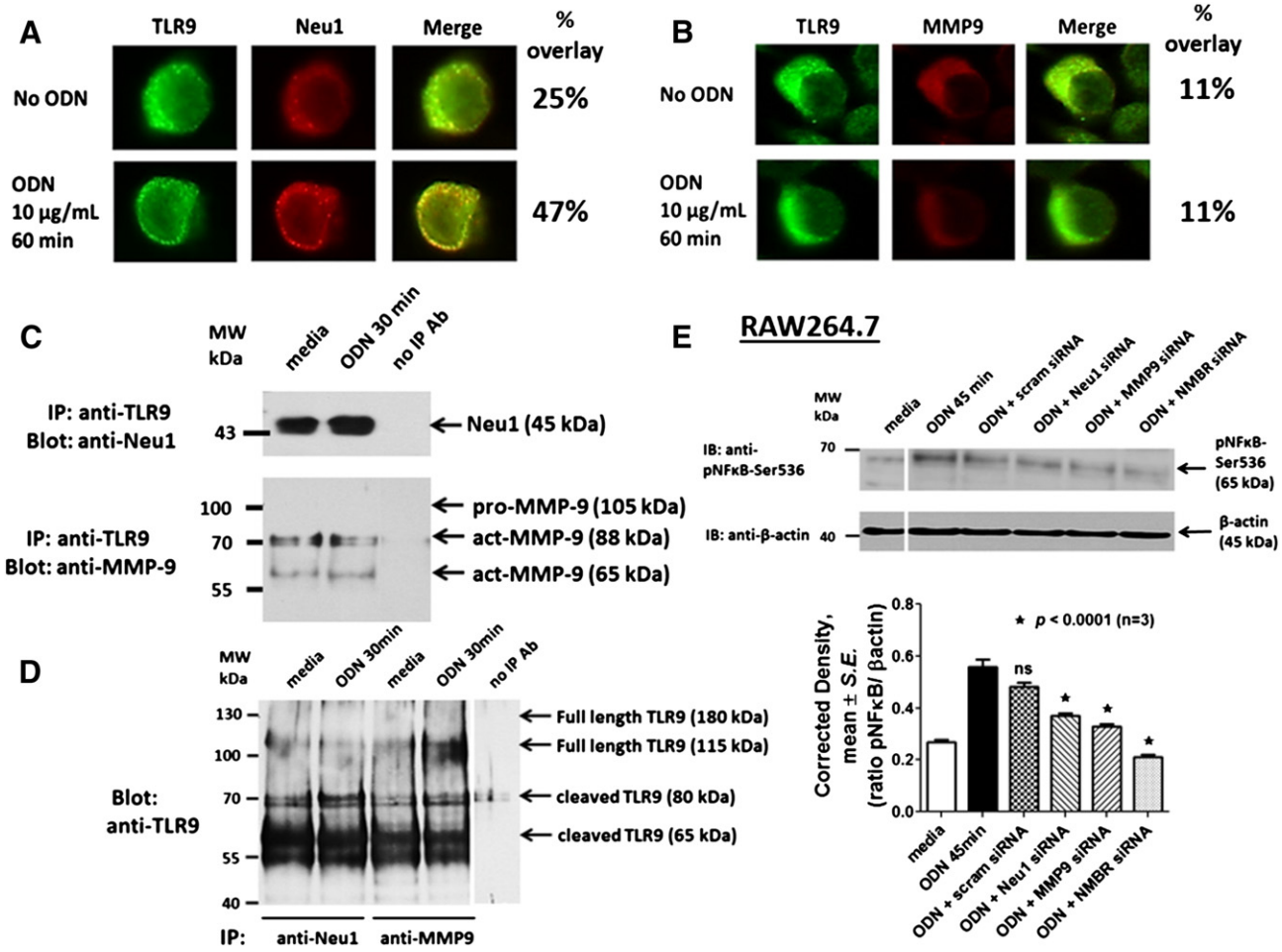

Fig. 4. (A) Neu1 and (B) MMP9 colocalize with TLR9. RAW-blue cells (50,000 cells) were plated on 12 mm circular glass slides in culture media containing 10% fetal calf sera for 24 h and treated with 10 μg/mL ODN for 60 min or left untreated as controls. Cells were fixed, permeabilized and immunostained with rabbit anti-TLR9, goat anti-Neu1 or goat anti-MMP9 followed with Alexa Fluor488 donkey anti-rabbit IgG or Alexa Fluor594 donkey anti-goat IgG. Stained cells were visualized using a Zeiss M2 imager with a 40× objective. To calculate the percentage of colocalization in the selected images, the Pearson correlation coefficient was measured on a total of 15–20 cells per image and expressed as a percentage using Image J 1.38x software. The data are a representation of one of three independent experiments showing similar results. (C) Neu1 and MMP9 co-immunoprecipitate with TLR9 and conversely (D) TLR9 co-IPs with Neu1 and MMP9. RAW-blue cells are left cultured in media or in media containing 10 μg/mL imiquimod for 30 min. Cells (1×10^7 cells) are pelleted and lysed in lysis buffer. TLR9, Neu1 or MMP9 in cell lysates from the cells are immunoprecipitated with 1.0 μg of rabbit anti-TLR9, rabbit anti-Neu1 or rabbit anti-MMP9 antibodies for 24 h. Following immunoprecipitation, complexes are isolated using protein A or G magnetic beads and resolved by 8% SDS-PAGE. The blots were probed for MMP9, Neu1 or TLR9 with specific antibodies followed by Clean-Blot IP Detection Reagent for IP/Western blots and Western Lightning Chemiluminescence Reagent Plus. The chemiluminescence reaction was analyzed with X-ray film. Sample concentration for gel loading was determined by Bradford assay. The data are a representation of one of three independent experiments showing similar results. (E) Western blot analysis of ODN-induced phosphorylated NF-κB (Ser(P)^{536}) in cell lysates from WT and siRNA knockdown (KD) RAW264.7 macrophage cells. WT cells and RAW264.7 siRNA KD Neu1, KD MMP9, KD NMBR and scrambled siRNA cells were treated with 10 μg/mL ODN for 45 min. Cell lysates from the WT and KD cells were separated by SDS-PAGE, and the blot was probed with phospho-specific polyclonal rabbit antibody against NF-κBp65-Ser(P)^{536}. β-Actin was used as an internal control protein for loading of the cytoplasmic cell lysate. Quantitative analysis was done by assessing the density of a band corrected for background in each lane using Corel Photo Paint 8.0 software. Each bar in the graphs represents the mean ratio of NF-κBp65-Ser(P)^{536} to β-actin of band density ± *S.E.* (error bars) for 3 independent measurements. *p* values represent significant differences at 99.9% confidence using the Dunnett's multiple comparison test compared with ligand-treated control cells.

3.8. Tamiflu, MMP9i and the heterotrimeric G-protein complex antagonist, BIM-46174 significantly abrogates imiquimod- and ODN-induced pro-inflammatory cytokines

To further confirm the signaling platform of Neu1 and MMP9 cross-talk in alliance with NMBR GPCR in regulating nucleic acid sensing TLR-7 and -9 receptors, we assessed the Bio-Plex cytokine microarray profiles in the tissue culture supernatants using the multiplex bead-based assay which is designed to quantitate multiple cytokines in single samples. The Bio-Plex suspension array system incorporates a novel technology using color-coded beads, which permits the simultaneous detection of cytokines in a single well of a 96-well microplate. The 96-well microplate-format Bio-Plex assays are optimized for the Bio-Plex suspension array system which utilizes xMAP detection technology. By multiplexing, it is possible to quantitate the level of multiple cytokines in a single well of tissue culture sample. Here, the chemokine (C–C motif) ligand 2 (CCL2) also referred to as monocyte chemotactic protein-1 (MCP-1) and TNFα were analyzed in tissue culture supernatants after 24 h stimulation of RAW-blue cells with either imiquimod or ODN. Tamiflu, MMP9i and the heterotrimeric G-protein complex antagonist, BIM-46174 significantly and dose-dependently abrogated MCP-1 and TNFα secretion associated with imiquimod- (Fig. 7A) and ODN- (Fig. 7B) stimulated RAW-blue cells after 24 h.

4. Discussion

The precise molecular mechanism(s) by which nucleic acid sensing TOLL-like receptors are activated is not well understood. For the majority of cell-surface TLR receptors, dimerization is a prerequisite

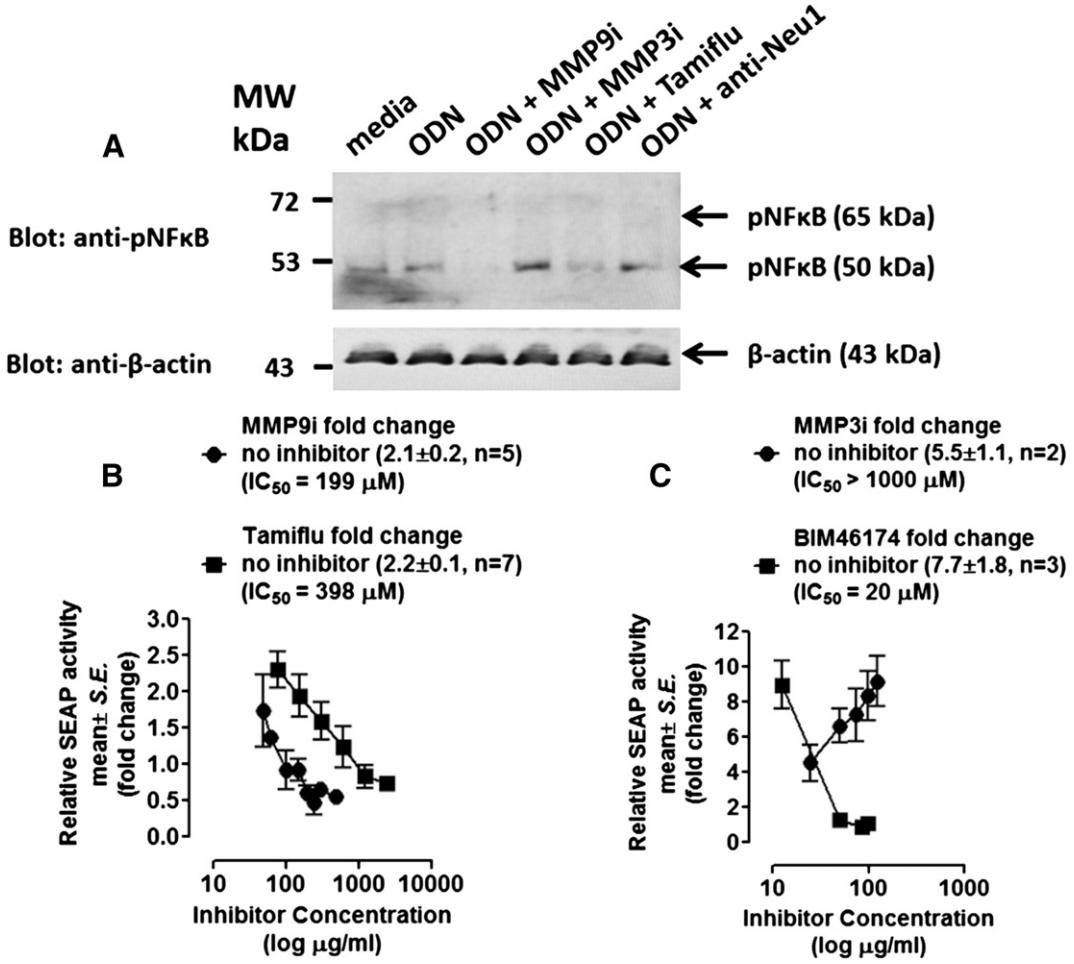

Fig. 5. (A) Western blot analysis of ODN-induced phosphorylated NF-κB-Ser(P)^{311} in cytoplasmic cell lysates from RAW-blue cells. Cells were pretreated with 200 μM Tamiflu, 100 μg/mL MMP9i, 100 μg/mL MMP3i or 50 μg/mL anti-Neu1 for 30 min followed by 10 μg/mL ODN or left untreated as medium control. Cell lysates were separated by SDS-PAGE, and the blot was probed with phospho-specific polyclonal rabbit antibody against NF-κB Ser(P)^{311}. β-Actin was used as internal control proteins for loading of the cytoplasmic cell lysate. The data are a representation of one of three independent experiments showing similar results. (B and C) Tamiflu, MMP9i and BIM46174 but not MMP3i dose-dependently NF-κB-dependent SEAP activity associated with ODN-treated SEAP reporter-expressing RAW-blue cells. Cells (1×10^5 cells) were treated with different doses of MMP3i, MMP9i, Tamiflu, and BIM46174 for 24 h, and SEAP activity in the culture medium was assessed using QUANTI-Blue substrate. Relative SEAP activity was calculated as fold change of each compound (SEAP activity in medium from treated cells minus no cell background over SEAP activity in medium from untreated cells minus background). The SEAP activity in the absence of inhibitors is indicated. The 50% inhibition concentration (IC_{50}) for each inhibitor on SEAP activity induced by ODN was determined by plotting the decrease in SEAP activity against the log of the agent concentration. The data are a representation of mean ± *S.E.* (n = 2–7 independent experiments as indicated).

to facilitate MyD88/TLR complex formation and subsequent cellular signaling to activate NF-κB. For intracellular TLR3 receptors, they also form dimers upon interaction of dsRNA. In contrast, the intracellular TLR8 [46] and TLR9 [20,21] appear to exist as preformed naive signaling dimers. For TLR-9, it is proposed that nucleic acids binding to two distinct binding sites [21,47] in the ectodomain of the receptors induce conformational changes which enable subsequent signaling. For TLR7 however, the precise mechanism(s) of nucleic acid action on the receptors is unknown. In this report, we uncovered a receptor signaling platform by nucleic acid ligands binding to TLR-7 and -9, which is orchestrated by a novel Neu1 and MMP-9 cross-talk in alliance with neuromedin B (NMBR) GPCR. This signaling paradigm was elucidated to be essential for nucleic acid activation of intracellular TLR-7 and TLR-9 receptors. In addition, specific inhibition of Neu1, MMP9 and the heterotrimeric G-protein complex tethered to both TLR-7 and -9 receptors in live RAW-blue macrophage cells significantly abrogates pro-inflammatory cytokines MCP-1 and TNFα. Indeed, other studies have provided evidence to show that ODN induces TNFα and TNFR-II at the transcriptional level, and that these molecular players are involved in MMP9 expression in the supernatants derived from murine RAW264.7 macrophage cell line by a TLR9 and a serine/threonine-specific protein kinase B (Akt)-mediated mechanism [48,49]. This ODN-induced MMP9 expression fits well within our novel Neu-1 and MMP9 cross-talk regulating TLR9 receptors.

Other reports have shown that ODN stimulation of 95D human lung cancer cells induced the secretion of high-mobility group protein B1 (HMGB1) dose-dependently [37]. The 95D cancer cell response to HMGB1 stimulation alone or acting synergistic with ODN mediated a MyD88-dependent up-regulation of MMP2, MMP9 and cyclin-dependent kinase-2 (CDK2), which was critically dependent on 35 kDa transmembrane receptor for advanced glycation endproducts (RAGE) and TLR4 receptors [37]. If ODN-induces HMGB1 secretion in these cancer cells, it might be possible that HMGB1 may affect ODN-induced NFκB activation via a TLR4 intermediary in our macrophage cells. Other reports provide evidence that this may not be the case. Secreted HMGB1 can be a trigger of inflammation dependent on the complexes it forms with other molecules [50]. Pure recombinant HMGB1 has no proinflammatory activity but can form highly inflammatory complexes with ssDNA, LPS, IL-1, and nucleosomes, which interact with TLR9, TLR4, IL-1R, and TLR2 receptors, respectively [50]. Interestingly, Ivanov et al. have identified HMGB1 as an

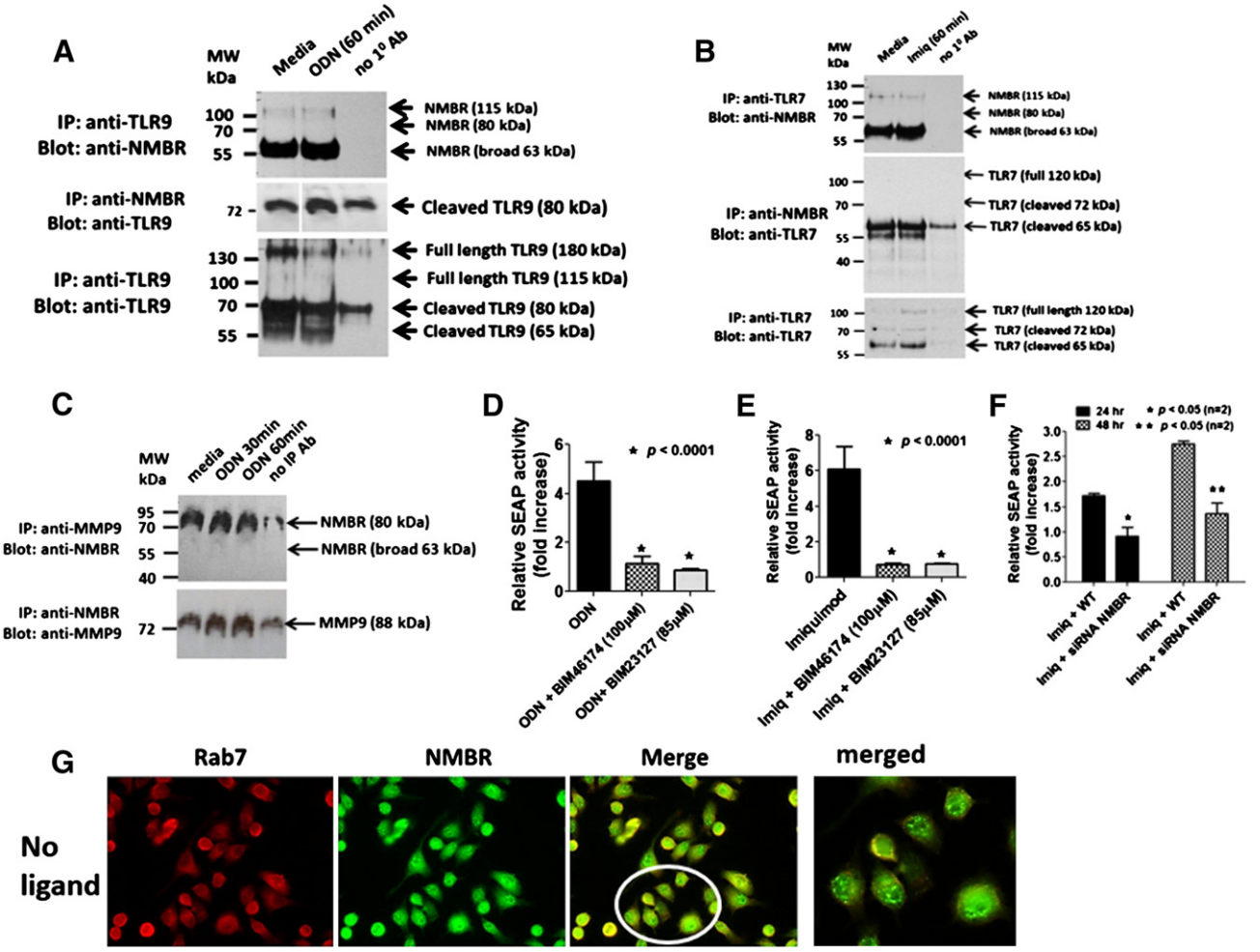

Fig. 6. Neuromedin B receptor (NMBR) co-immunoprecipitates with TLR9 (A) and TLR7 (B), and conversely, TLR7 and TLR9 co-IPs with NMBR. RAW-blue cells were left cultured in media or in media containing 10 μg/mL ODN or imiquimod for 60 min. Cells (1×10^7 cells) were pelleted and lysed in lysis buffer. NMBR and TLR-7 and -9 receptors in the cell lysates from the cells were immunoprecipitated with 1 μg of goat anti-NMBR, 1 μg of rabbit anti-TLR7 or rabbit anti-TLR9 antibodies for 24 h. Following immunoprecipitation, complexes were isolated using protein A or G magnetic beads, washed 3× in buffer and resolved by 8% SDS-PAGE. The blots were probed for NMBR with rabbit anti-NMBR or TLR7 or TLR9 with respective antibodies followed by Clean-Blot IP Detection Reagent for IP/Western blots and Western Lightning Chemiluminescence Reagent Plus. The chemiluminescence reaction was analyzed with X-ray film. Sample concentration for gel loading was determined by Bradford assay. The data are a representation of one of three independent experiments showing similar results. (C) NMBR co-immunoprecipitates with MMP9, and conversely, MMP9 co-IPs with NMBR in cell lysates from naive and ODN-treated RAW-blue cells. Cells were left cultured in media or in media containing 10 μg/mL ODN for 30 and 60 min. Cells (1×10^7 cells) were pelleted and lysed in lysis buffer. NMBR and MMP9 receptors in the cell lysates from the cells were immunoprecipitated with 1 μg of goat anti-NMBR or rabbit anti-TLR9 antibodies for 24 h. Immunoprecipitation was followed as described in (A). The data are a representation of one of two independent experiments showing similar results. BIM23127 and BIM-46174 inhibit (D) ODN- and (E) imiquimod-induced NF-κB-dependent SEAP activity in SEAP reporter-expressing RAW-Blue cells. Cells (1×10^5 cells) were treated with 85 μM BIM23127 or 100 μM BIM46174 plus indicated ligand for 24 h, and SEAP activity in the culture medium was assessed using QUANTI-Blue substrate. The data are the mean ± *S.E.* (*error bars*) of three independent experiments. *p* values represent significant differences at 99% confidence using the Dunnett's multiple comparison test compared with ligand-treated control cells. (F) siRNA NMBR KD RAW-blue cells inhibit NF-κB-dependent SEAP activity. WT and siRNA NMBR KD RAW-blue cells were treated with imiquimod for 24 h and SEAP activity in the culture medium was assessed using QUANTI-Blue substrate. Results are mean ± *S.E.* of three independent experiments. (G) NMBR colocalizes with Rab7. RAW-blue cells (50,000 cells) were plated on 12 mm circular glass slides in culture media containing 10% fetal calf sera for 24 h and left untreated. Cells were fixed, permeabilized and immunostained with rabbit anti-NMBR and mouse anti-Rab7 followed with Fluor568 donkey anti-mouse IgG or Alexa Fluor488 donkey anti-rabbit IgG. Stained cells were visualized using a Zeiss M2 imager with a 40× objective. To calculate the percentage of colocalization in the selected images, the Pearson correlation coefficient was measured on a total of 15–20 cells per image and expressed as a percentage using Image J 1.38x software. The data are a representation of one of two independent experiments showing similar results.

ODN-binding protein, and it interacts and pre-associates with TLR9 in the endoplasmic reticulum–Golgi intermediate compartment, hastening TLR9's redistribution to early endosomes in response to ODN [16]. Based on these data, the extracellular HMGB1 was found to accelerate the delivery of ODNs to its receptor, leading to a TLR9-dependent augmentation of IL-6, IL-12, and TNFα secretion [16]. Using the murine macrophage-like cell lines, RAW 264.7 and J774A.1, Pisetsky and colleagues have clearly shown that under conditions in which the ODN1826 activated the cell lines, as assessed by stimulation of tumor necrosis factor-α and interleukin-12, it failed to cause HMGB1 release into the media [38]. Although unable to induce HMGB1 release by itself, the ODN1826 nevertheless potentiated the action of LPS in these macrophage cells [38]. The findings in our studies are consistent with these reported studies demonstrating that TLR9 activation associated with ODN1826-treated macrophages, HEK-293 and HEK-TKR7-HA cells do not involve HMGB1-induced TLR4 as an intermediary.

We previously reported that Neu1 is an important intermediate in the initial process of cell surface TLR ligand-induced receptor activation and subsequent cellular function [23,24]. The data also provided evidence for a physiological relevance of Neu1 in regulating endotoxin LPS induced pro-inflammatory cytokines and nitric oxide production [24]. Using Neu1 deficient mice, serum pro-inflammatory cytokines were induced in wild-type (WT) and Neu1-deficient mice responding to LPS after 5 h treatment when compared to basal serum levels. However, the Neu1-deficient mice produced a

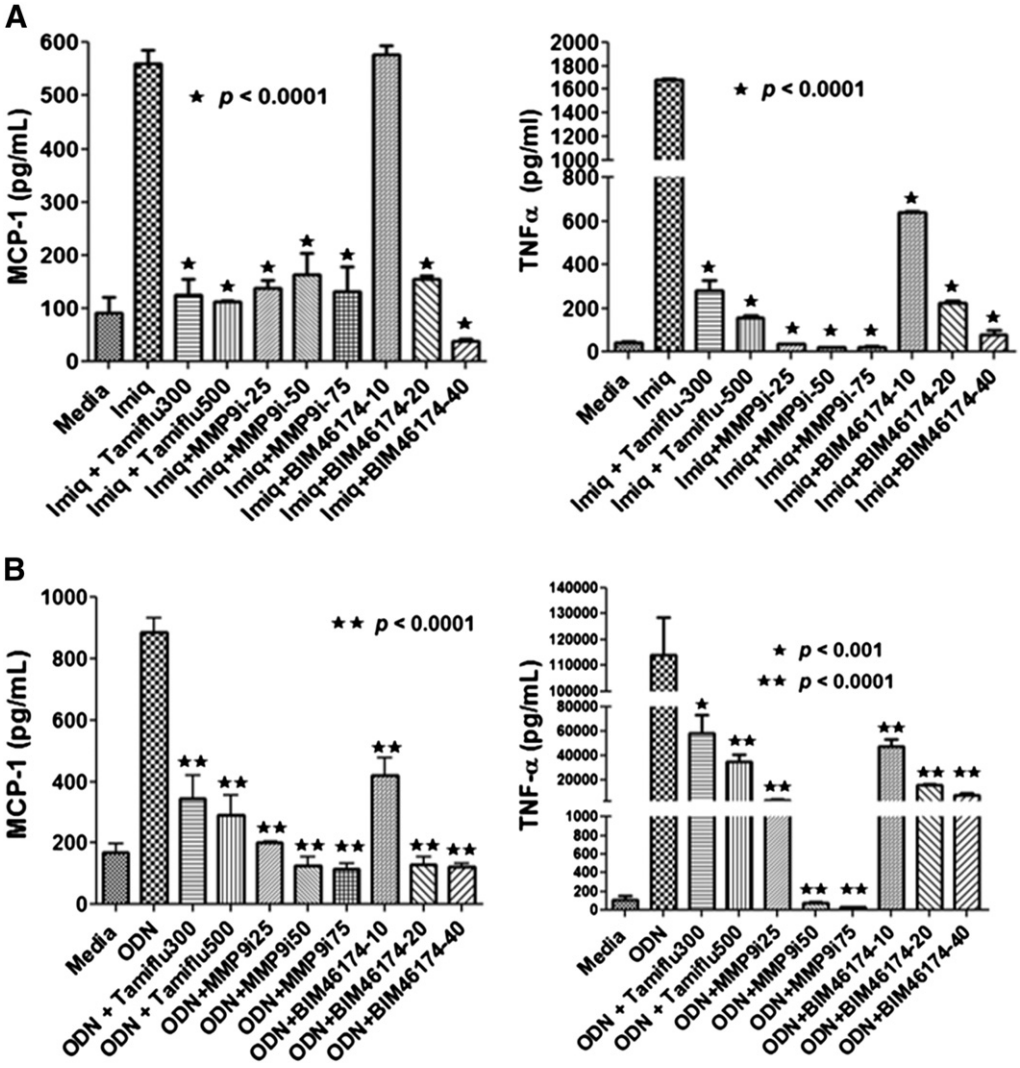

Fig. 7. Bio-Plex cytokine microarray profiles in the cell culture supernatants using the multiplex color-coded beads. RAW-blue cells were cultured in 96-well microplate at 30,000 cells per well for 24 h followed by pretreatment with Tamiflu, MMP9i and BIM-46174 at the indicated doses in μg/mL for 1 h. The pretreated cells were stimulated for 24 h with either 20 μg/mL imiquimod (A) or 20 μg/mL ODN (B). The Bio-Plex suspension array system was optimized using the xMAP detection technology. The quantitation of the level of TNFα and MCP-1 cytokines in a single well of tissue culture sample was assessed from a standard curve. Each bar in the graphs represents the mean ± *S.E.* (error bars) of three separate experiments. *p* values represent significant differences at 99% confidence intervals using the Dunnett's multiple comparison test compared with ligand-treated positive controls.

significant diminution in C5a, G-CFS, IL-1ra, IL-6, KC (cytokine induced neutrophil chemo-attractant) and MIP2 (macrophage inflammatory protein-2) cytokines in response to LPS compared to the wild-type mice. Using an IL-6 ELISA assay, serum IL-6 was significantly reduced in LPS treated Neu1 deficient mice compared to the WT. The neuraminidase inhibitor Tamiflu treatment of human monocytic THP-1 cells dose-dependently inhibited IL-6 and TNFα production in response to LPS [24]. Flow cytometric analyses confirmed this to be the case, suggesting that inhibition of the Neu1 sialidase activity by Tamiflu is able to significantly inhibit LPS induced pro-inflammatory cytokine IL-6 and TNFα production dose-dependently. In addition, Tamiflu significantly inhibited the production of nitric oxide (NO) in DC2.4 dendritic cells following LPS or killed *Mycobacterium butyricum* stimulation. Primary bone marrow (BM) macrophage cells from Neu1-deficient mice exhibited a significant reduction in endotoxin LPS-induced NO production in comparison to WT cohort. Primary BM macrophage cells derived CathA KI mice (normal Neu1 and inactive cathepsin A) or Neu4 knockout (KO) mice exhibited LPS induced NO production comparable to the WT cohort [24]. Collectively, proinflammatory IL-6 and TNFα cytokines and nitric oxide production associated with endotoxin LPS activation of cell surface TLR4 receptors are partially dependent on Neu1 sialidase in conjugation with MMP-9 and GPCR signaling [24,35]. The data in this report provide further evidence to support an identical signaling platform in regulating nucleic acid-induced endosomal TLRs to produce TNFα and MCP-1 cytokines.

It has become evident that TLRs require additional proteins to be activated by their respective ligands. For an example, not only is CD14 associated with MyD88-dependent TLR4 receptors on the cell surface, but it also constitutively interacts with the MyD88-dependent TLR7 and TLR9 receptors [51]. It was found that CD14 was necessary for TLR7- and TLR9-dependent induction of proinflammatory cytokines in vitro and for TLR9-dependent innate immune responses in mice. In addition, the absence of CD14 led to reduced nucleic acid uptake in macrophages. Using various types of vesicular stomatitis virus, the report showed that CD14 is dispensable for viral uptake but is required for the triggering of TLR-dependent cytokine responses [51]. These findings suggest that CD14 has a dual role in nucleic acid-mediated TLR activation whereby it can promote the selective uptake of nucleic acids, and at the same time, it acts as a co-receptor for endosomal TLR activation. Interestingly, others have demonstrated another important role for CD14 [52]. It also associates with Gi (inhibitory class) and Go (olfactory class) α subunits of G-proteins. The heterotrimeric G proteins were shown to have a

specific regulatory function in CD14-associated LPS-induced mitogen-activated protein kinase (MAPK) activation and cytokine production in normal human monocytes [52]. A significant decrease in LPS-induced activation of c-Jun-N-terminal kinase (JNK) and p38 kinase was reported with a subsequent loss in the production of TNF-α when THP-1 human monocyte cells were pretreated with Gαi-sensitive pertussis toxin [53]. Using the knockout mouse models of $G\alpha_{i2}^{-/-}$ and $G\alpha_{i1/3}^{-/-}$ proteins, Fan et al. [54] showed a significant decrease in TLR ligand-mediated TNF-α and IL-10 production in peritoneal macrophages of the knockout mice compared to wild-type cohort. These findings suggest a regulatory role for Gαi proteins in TLR signaling, which is potentially dependent on a cellular phenotype [55]. In the murine RAW 264.7 macrophage cell line and primary murine macrophages, G protein dysregulation induced by wasp venom-derived peptide mastoparan caused a significant inhibition in LPS-induced TLR4-, but not in TLR2-mediated gene expression [56]. The data in the present report support a unique organizational GPCR signaling platform as the initial processing stage for GPCR signaling in mediating MMP9 activation to induce Neu1, all of which form a tripartite complex with TLR-7 and -9 receptors. This signaling paradigm was essential for subsequent downstream cellular signaling and the production of pro-inflammatory cytokines. In the present report, the involvement of heterotrimeric G-protein complex in TLR ligand-mediated receptor function has also been shown for endosomal TLRs. Using siRNA NMBR knockdown cells and neuromedin B receptor antagonist BIM-23127 and the heterotrimeric G-protein complex antagonist BIM-46174, the results provided evidence for a significant diminution of NF-κB activation and reduced MyD88 recruitment associated with imiquimod- and ODN- stimulated RAW-blue cells. Collectively, the data validated the predicted alliance between nucleic acid sensing TLR-7 and -9 receptors and NMBR GPCR localized in the late endocytic lysosomal pathway of naive macrophage cells. This TLR signaling paradigm also predicts that endosomal TLR receptors are in alliance with a functional GPCR signaling complex.

In support of this premise, our studies and others have provided important evidence to show that the crosstalk between GPCR and TLR signaling pathways and the GPCR signaling molecules may have uncharacterized functions in macrophage cells [1–3,57]. Recently, we have reported that GPCR agonists bombesin, bradykinin, lysophosphatidic acid (LPA), cholesterol, angiotensin-1 and -2, but not thrombin induce Neu1 activity in live macrophage cell lines and primary bone marrow macrophage cells from wild-type (WT) mice but not from Neu1-deficient mice [3]. Using immunocytochemistry and NFκB-dependent secretory alkaline phosphatase (SEAP) analyses, bombesin induced NFκB activation in BMC-2 and RAW-blue macrophage cells, which was inhibited by MyD88 homodimerization inhibitor, Tamiflu, galardin, piperazine and anti-MMP-9 antibody [3]. The bombesin-related receptor, neuromedin B (NMBR), formed a complex with TLR4 and MMP9. Silencing MMP9 mRNA using siRNA transfection of RAW-blue macrophage cells markedly reduced Neu1 activity associated with bombesin-, bradykinin- and LPA-treated cells compared to the untreated controls [3]. Interestingly, the data in the report indicated that the three different isoforms of NMBR are tethered to TLR-4 receptors, but it was the 80 kDa isoform of NMBR which formed a complex with MMP-9, making it readily available to activate MMP-9 on the cell surface of naive macrophage cells. Unexpectedly, the 63 and 80 kDa isoforms of NMBR are eventually lost over time with LPS treatment. In the present study, we have found that the 63 kDa isoform of NMBR is also tethered to the cleaved 65 kDa TLR-7 and the cleaved 80 kDa TLR9 receptors with no loss with ligand-stimulation of the cells over 60 min. The reason(s) for this differential activity of the NMBR isoforms is unknown. More importantly, the similarity of the mechanism NMBR in alliance with Neu1 and MMP9 regulating TLR4 on the cell surface and the intracellular TLR7 and TLR9 in the endosomal compartments is striking. The data shown in Fig. 1 suggest that the MMP9/Neu1 complex is separately tethered to either TLR-4, -7 or -9 receptors and it does not shuttle from the cell surface to the endosomal compartments and vice-versa. Firstly, the NMBR/MMP9/Neu1 tripartite complex is already present on TLR4 [2] and TLR-7 and -9 receptors in naive, unstimulated cells. Secondly, imiquimod and ODN stimulation of HEK-293 and HEK-TLR7-HA induce NFκB activation in the absence of the TLR4 intermediary. What we do not understand is how and when this novel regulatory signaling complex is formed on these receptors.

The connection between NMBR GPCR and Neu1/MMP9 is intriguing. The diverse multiple actions of GPCRs regulating TLRs and its translation to human disease require further investigations to uncover their functional roles in cellular signaling [1]. Accordingly, the regulation and sorting of GPCRs by endocytic membrane trafficking and its potential implications are eloquently reviewed by Hanyaloglu and colleagues [58,59] and Marchese et al. [60]. Indeed, achieving a coordinated regulation of multiple receptor-mediated signaling is one of the mandates for GPCRs which represent the largest family of signaling receptors expressed in animals, and they respond to a wide range of stimuli. The evidence suggests an unprecedented degree of specificity and plasticity in the cellular regulation of mammalian GPCRs by endocytic membrane trafficking [58]. The diverse physiological roles played by GPCRs are noteworthy of further study. For examples, there is evidence for disordered GPCR signaling in various pathological conditions such as (a) dysregulation of GPCR function [61], (b) the 'loss of function' mutation or the 'gain of function' mutation [62], (c) constitutively active GPCRs especially those that are tumorigenic in vitro and in animal models of human disease that cause syndromes of hyperfunction and/or tumors in humans including diseases involving infectious viral agents [61,63] and (d) the mutant GPCRs as a cause of human diseases [64]. To date, over 600 inactivating and almost 100 activating mutations in GPCR have been identified, which are responsible for more than 30 different human diseases. The number of human disorders is expected to increase given the fact that over 160 GPCRs have been targeted in mice [64].

Perhaps, one mechanism by which ligand-induced TLR activation could modify GPCR signaling is by altering the expression of regulator of G protein signaling (RGS) proteins [65]. Other reports have shown that GPCR sphingosine 1-phosphate S1P1 and S1P3 expression was induced by LPS in human gingival epithelial cells (HGEC), and this elevated expression enhanced the influence of S1P in its cooperation with TLR4 to increase cytokine production [66]. Furthermore, the relationship between GPCR-signaling and TLR has been shown for (a) CC chemokine ligand-2 synergizing with the non-chemokine GPCR ligand fMLP in monocyte chemotaxis [67], (b) beta-arrestin 2 involvement in complement C1q expression in macrophages [68], (c) leukotriene B4 (LTB4) receptor BTL1 reduction of SOCS1 inhibition of MyD88 expression in mouse macrophages [69] and (d) GPCR-derived cAMP signaling influencing TLR responses in primary macrophages through peptide disruptors of A-kinase anchoring protein (AKAP10) involving prostaglandin E2 (PGE2) [70].

Collectively, the parameters controlling interactions between the TLRs and their ligands still remain poorly defined. The present report proposes that Neu1 is an important intermediate in the initial process of endosomal TLR nucleic acid-induced receptor activation and subsequent cellular function. Central to this process is that Neu1 and MMP9 in alliance with the 63 kDa isoform of GPCR NMBR receptor are separately tethered to TLR-7 and -9 receptors in naive TLR-expressing cells. This paradigm signifies an unprecedented molecular GPCR signaling platform of a Neu1 and MMP9 cross-talk in alliance with endosomal TLR-7 and -9 that is essential for nucleic acid activation of endosomal TLRs and subsequent cellular signaling.

Competing financial interests

The authors declare no competing financial interests.

Acknowledgments

These studies are supported by a grant to M.R.S. from the Natural Sciences and Engineering Research Council of Canada (NSERC). S.A. was the recipient of the R.S. McLaughlin Scholarship, the Ontario Graduate Scholarship and now, the Canadian Institutes of Health Research (CIHR) Doctoral Award: Frederick Banting and Charles Best Canada Graduate Scholarship.

References

[1] S. Abdulkhalek, M. Hrynyk, M.R. Szewczuk, Research and Reports in Biochemistry 3 (2013) 17–30.
[2] S. Abdulkhalek, S.R. Amith, S.L. Franchuk, P. Jayanth, M. Guo, T. Finlay, A. Gilmour, C. Guzzo, K. Gee, R. Beyaert, M.R. Szewczuk, The Journal of Biological Chemistry 286 (42) (2011) 36532–36549.
[3] S. Abdulkhalek, M. Guo, S.R. Amith, P. Jayanth, M.R. Szewczuk, Cellular Signalling 24 (11) (2012) 2035–2042.
[4] C.R. Stewart, L.M. Stuart, K. Wilkinson, J.M. van Gils, J. Deng, A. Halle, K.J. Rayner, L. Boyer, R. Zhong, W.A. Frazier, A. Lacy-Hulbert, J. El Khoury, D.T. Golenbock, K.J. Moore, Nature Immunology 11 (2) (2010) 155–161.
[5] K. Hoebe, P. Georgel, S. Rutschmann, X. Du, S. Mudd, K. Crozat, S. Sovath, L. Shamel, T. Hartung, U. Zahringer, B. Beutler, Nature 433 (7025) (2005) 523–527.
[6] K. Miyake, International Immunopharmacology 3 (1) (2003) 119–128.
[7] R. Shimazu, S. Akashi, H. Ogata, Y. Nagai, K. Fukudome, K. Miyake, M. Kimoto, The Journal of Experimental Medicine 189 (11) (1999) 1777–1782.
[8] A. Visintin, E. Latz, B.G. Monks, T. Espevik, D.T. Golenbock, The Journal of Biological Chemistry 278 (48) (2003) 48313–48320.
[9] A.L. Blasius, B. Beutler, Immunity 32 (3) (2010) 305–315.
[10] F. Randow, B. Seed, Nature Cell Biology 3 (10) (2001) 891–896.
[11] K. Takahashi, T. Shibata, S. Akashi-Takamura, T. Kiyokawa, Y. Wakabayashi, N. Tanimura, T. Kobayashi, F. Matsumoto, R. Fukui, T. Kouro, Y. Nagai, K. Takatsu, S. Saitoh, K. Miyake, The Journal of Experimental Medicine 204 (12) (2007) 2963–2976.
[12] Y. Wakabayashi, M. Kobayashi, S. Akashi-Takamura, N. Tanimura, K. Konno, K. Takahashi, T. Ishii, T. Mizutani, H. Iba, T. Kouro, S. Takaki, K. Takatsu, Y. Oda, Y. Ishihama, S. Saitoh, K. Miyake, The Journal of Immunology 177 (3) (2006) 1772–1779.
[13] K. Konno, Y. Wakabayashi, S. Akashi-Takamura, T. Ishii, M. Kobayashi, K. Takahashi, Y. Kusumoto, S. Saitoh, Y. Yoshizawa, K. Miyake, Biochemical and Biophysical Research Communications 339 (4) (2006) 1076–1082.
[14] K. Tabeta, K. Hoebe, E.M. Janssen, X. Du, P. Georgel, K. Crozat, S. Mudd, N. Mann, S. Sovath, J. Goode, L. Shamel, A.A. Herskovits, D.A. Portnoy, M. Cooke, L.M. Tarantino, T. Wiltshire, B.E. Steinberg, S. Grinstein, B. Beutler, Nature Immunology 7 (2) (2006) 156–164.
[15] M.M. Brinkmann, E. Spooner, K. Hoebe, B. Beutler, H.L. Ploegh, Y.M. Kim, The Journal of Cell Biology 177 (2) (2007) 265–275.
[16] S. Ivanov, A.M. Dragoi, X. Wang, C. Dallacosta, J. Louten, G. Musco, G. Sitia, G.S. Yap, Y. Wan, C.A. Biron, M.E. Bianchi, H. Wang, W.M. Chu, Blood 110 (6) (2007) 1970–1981.
[17] C. Iavarone, K. Ramsauer, A.V. Kubarenko, J.C. Debasitis, I. Leykin, A.N. Weber, O.M. Siggs, B. Beutler, P. Zhang, G. Otten, U. D'Oro, N.M. Valiante, M.L. Mbow, A. Visintin, The Journal of Immunology 186 (7) (2011) 4213–4222.
[18] J.K. Bell, J. Askins, P.R. Hall, D.R. Davies, D.M. Segal, Proceedings of the National Academy of Sciences of the United States of America 103 (23) (2006) 8792–8797.
[19] J.K. Bell, I. Botos, P.R. Hall, J. Askins, J. Shiloach, D.M. Segal, D.R. Davies, Proceedings of the National Academy of Sciences of the United States of America 102 (31) (2005) 10976–10980.
[20] E. Latz, A. Verma, A. Visintin, M. Gong, C.M. Sirois, D.C. Klein, B.G. Monks, C.J. McKnight, M.S. Lamphier, W.P. Duprex, T. Espevik, D.T. Golenbock, Nature Immunology 8 (7) (2007) 772–779.
[21] M.E. Peter, A.V. Kubarenko, A.N. Weber, A.H. Dalpke, The Journal of Immunology 182 (12) (2009) 7690–7697.
[22] A. Woronowicz, K. De Vusser, W. Laroy, R. Contreras, S.O. Meakin, G.M. Ross, M.R. Szewczuk, Glycobiology 14 (11) (2004) 987–998.
[23] S.R. Amith, P. Jayanth, S. Franchuk, T. Finlay, V. Seyrantepe, R. Beyaert, A.V. Pshezhetsky, M.R. Szewczuk, Cellular Signalling 22 (2) (2010) 314–324.
[24] S.R. Amith, P. Jayanth, S. Franchuk, S. Siddiqui, V. Seyrantepe, K. Gee, S. Basta, R. Beyaert, A.V. Pshezhetsky, M.R. Szewczuk, Glycoconjugate Journal 26 (9) (2009) 1197–1212.
[25] A. Woronowicz, S.R. Amith, V.W. Davis, P. Jayanth, K. De Vusser, W. Laroy, R. Contreras, S.O. Meakin, M.R. Szewczuk, Glycoconjugate Journal 17 (7) (2007) 725–734.
[26] P. Jayanth, S.R. Amith, K. Gee, M.R. Szewczuk, Cellular Signalling 22 (8) (2010) 1193–1205.
[27] A. Woronowicz, S.R. Amith, K. De Vusser, W. Laroy, R. Contreras, S. Basta, M.R. Szewczuk, Glycobiology 17 (1) (2007) 10–24.
[28] S.E. Ewald, B.L. Lee, L. Lau, K.E. Wickliffe, G.P. Shi, H.A. Chapman, G.M. Barton, Nature 456 (7222) (2008) 658–662.
[29] B. Park, M.M. Brinkmann, E. Spooner, C.C. Lee, Y.M. Kim, H.L. Ploegh, Nature Immunology 9 (12) (2008) 1407–1414.
[30] M. Asagiri, T. Hirai, T. Kunigami, S. Kamano, H.J. Gober, K. Okamoto, K. Nishikawa, E. Latz, D.T. Golenbock, K. Aoki, K. Ohya, Y. Imai, Y. Morishita, K. Miyazono, S. Kato, P. Saftig, H. Takayanagi, Science 319 (5863) (2008) 624–627.
[31] R. Fukui, S. Saitoh, F. Matsumoto, H. Kozuka-Hata, M. Oyama, K. Tabeta, B. Beutler, K. Miyake, The Journal of Experimental Medicine 206 (6) (2009) 1339–1350.
[32] F. Matsumoto, S. Saitoh, R. Fukui, T. Kobayashi, N. Tanimura, K. Konno, Y. Kusumoto, S. Akashi-Takamura, K. Miyake, Biochemical and Biophysical Research Communications 367 (3) (2008) 693–699.
[33] F.E. Sepulveda, S. Maschalidi, R. Colisson, L. Heslop, C. Ghirelli, E. Sakka, A.M. Lennon-Dumenil, S. Amigorena, L. Cabanie, B. Manoury, Immunity 31 (5) (2009) 737–748.
[34] S. Maschalidi, S. Hassler, F. Blanc, F.E. Sepulveda, M. Tohme, M. Chignard, P. van Endert, M. Si-Tahar, D. Descamps, B. Manoury, PLoS Pathogens 8 (8) (2012) e1002841.
[35] T.M. Finlay, S. Abdulkhalek, A. Gilmour, C. Guzzo, P. Jayanth, S.R. Amith, K. Gee, R. Beyaert, M.R. Szewczuk, Glycoconjugate Journal 27 (6) (2010) 583–600.
[36] T.M. Finlay, P. Jayanth, S.R. Amith, A. Gilmour, C. Guzzo, K. Gee, R. Beyaert, M.R. Szewczuk, Glycoconjugate Journal 27 (3) (2010) 329–348.
[37] C. Wang, G. Fei, Z. Liu, Q. Li, Z. Xu, T. Ren, Cancer Biology & Therapy 13 (9) (2012) 727–736.
[38] W. Jiang, J. Li, M. Gallowitsch-Puerta, K.J. Tracey, D.S. Pisetsky, Journal of Leukocyte Biology 78 (4) (2005) 930–936.
[39] G.P. Prevost, M.O. Lonchampt, S. Holbeck, S. Attoub, D. Zaharevitz, M. Alley, J. Wright, M.C. Brezak, H. Coulomb, A. Savola, M. Huchet, S. Chaumeron, Q.D. Nguyen, P. Forgez, E. Bruyneel, M. Bracke, E. Ferrandis, P. Roubert, D. Demarquay, C. Gespach, P.G. Kasprzyk, Cancer Research 66 (18) (2006) 9227–9234.
[40] O.M. Fischer, S. Hart, A. Ullrich, Methods in Molecular Biology 327 (2006) 85–97.
[41] S.M. Le Gall, R. Auger, C. Dreux, P. Mauduit, The Journal of Biological Chemistry 278 (46) (2003) 45255–45268.
[42] S. Murasawa, Y. Mori, Y. Nozawa, N. Gotoh, M. Shibuya, H. Masaki, K. Maruyama, Y. Tsutsumi, Y. Moriguchi, Y. Shibazaki, Y. Tanaka, T. Iwasaka, M. Inada, H. Matsubara, Circulation Research 82 (12) (1998) 1338–1348.
[43] T. Haas, J. Metzger, F. Schmitz, A. Heit, T. Muller, E. Latz, H. Wagner, Immunity 28 (3) (2008) 315–323.
[44] D. Calebiro, V.O. Nikolaev, M.J. Lohse, Journal of Molecular Endocrinology 45 (1) (2010) 1–8.
[45] D. Calebiro, V.O. Nikolaev, L. Persani, M.J. Lohse, Trends in Pharmacological Sciences 31 (5) (2010) 221–228.
[46] J. Zhu, R. Brownlie, Q. Liu, L.A. Babiuk, A. Potter, G.K. Mutwiri, Molecular Immunology 46 (5) (2009) 978–990.
[47] M. Rutz, J. Metzger, T. Gellert, P. Luppa, G.B. Lipford, H. Wagner, S. Bauer, European Journal of Immunology 34 (9) (2004) 2541–2550.
[48] E.J. Lim, S.H. Lee, J.G. Lee, B.R. Chin, Y.S. Bae, J.R. Kim, C.H. Lee, S.H. Baek, FEBS Letters 580 (18) (2006) 4533–4538.
[49] E.J. Lim, S.H. Lee, J.G. Lee, J.R. Kim, S.S. Yun, S.H. Baek, C. Lee, Experimental & Molecular Medicine 39 (2) (2007) 239–245.
[50] M.E. Bianchi, Journal of Leukocyte Biology 86 (3) (2009) 573–576.
[51] C.L. Baumann, I.M. Aspalter, O. Sharif, A. Pichlmair, S. Bluml, F. Grebien, M. Bruckner, P. Pasierbek, K. Aumayr, M. Planyavsky, K.L. Bennett, J. Colinge, S. Knapp, G. Superti-Furga, The Journal of Experimental Medicine 207 (12) (2010) 2689–2701.
[52] K.R. Solomon, E.A. Kurt-Jones, R.A. Saladino, A.M. Stack, I.F. Dunn, M. Ferretti, D. Golenbock, G.R. Fleisher, R.W. Finberg, The Journal of Clinical Investigation 102 (11) (1998) 2019–2027.
[53] M. Ferlito, O.G. Romanenko, K. Guyton, S. Ashton, F. Squadrito, P.V. Halushka, J.A. Cook, Journal of Endotoxin Research 8 (6) (2002) 427–435.
[54] H. Fan, B. Zingarelli, O.M. Peck, G. Teti, G.E. Tempel, P.V. Halushka, K. Spicher, G. Boulay, L. Birnbaumer, J.A. Cook, American Journal of Physiology. Cell Physiology 289 (2) (2005) C293–C301.
[55] H.K. Fan, B. Zingarelli, O.M. Peck, G. Teti, G.E. Tempel, P.V. Halushka, J.A. Cook, American Journal of Physiology. Cell Physiology 289 (2) (2005) C293–C301.
[56] D. Li, H. Ji, S. Zaghlul, K. McNamara, M.C. Liang, T. Shimamura, S. Kubo, M. Takahashi, L.R. Chirieac, R.F. Padera, A.M. Scott, A.A. Jungbluth, W.K. Cavenee, L.J. Old, G.D. Demetri, K.K. Wong, The Journal of Clinical Investigation 117 (2) (2007) 346–352.
[57] J. Lattin, D.A. Zidar, K. Schroder, S. Kellie, D.A. Hume, M.J. Sweet, Journal of Leukocyte Biology 82 (1) (2007) 16–32.
[58] A.C. Hanyaloglu, M. von Zastrow, Annual Review of Pharmacology and Toxicology 48 (2008) 537–568.
[59] F. Jean-Alphonse, A.C. Hanyaloglu, Molecular and Cellular Endocrinology 331 (2) (2011) 205–214.
[60] A. Marchese, M.M. Paing, B.R. Temple, J. Trejo, Annual Review of Pharmacology and Toxicology 48 (2008) 601–629.
[61] L. Arvanitakis, E. Geras-Raaka, M.C. Gershengorn, Trends in Endocrinology and Metabolism 9 (1) (1998) 27–31.
[62] A.M. Spiegel, L.S. Weinstein, Annual Review of Medicine 55 (2004) 27–39.
[63] Y.X. Tao, Pharmacology & Therapeutics 120 (2) (2008) 129–148.
[64] T. Schoneberg, A. Schulz, H. Biebermann, T. Hermsdorf, H. Rompler, K. Sangkuhl, Pharmacology & Therapeutics 104 (3) (2004) 173–206.
[65] G.X. Shi, K. Harrison, S.B. Han, C. Moratz, J.H. Kehrl, The Journal of Immunology 172 (9) (2004) 5175–5184.
[66] M.A. Eskan, B.G. Rose, M.R. Benakanakere, Q. Zeng, D. Fujioka, M.H. Martin, M.J. Lee, D.F. Kinane, European Journal of Immunology 38 (4) (2008) 1138–1147.
[67] M. Gouwy, S. Struyf, H. Verbeke, W. Put, P. Proost, G. Opdenakker, J. Van Damme, Journal of Leukocyte Biology 86 (3) (2009) 671–680.
[68] J.E. Lattin, K.P. Greenwood, N.L. Daly, G. Kelly, D.A. Zidar, R.J. Clark, W.G. Thomas, S. Kellie, D.J. Craik, D.A. Hume, M.J. Sweet, Molecular Immunology 47 (2–3) (2009) 340–347.
[69] C.H. Serezani, C. Lewis, S. Jancar, M. Peters-Golden, The Journal of Clinical Investigation 121 (2) (2011) 671–682.
[70] S.H. Kim, C.H. Serezani, K. Okunishi, Z. Zaslona, D.M. Aronoff, M. Peters-Golden, The Journal of Biological Chemistry 286 (2011) 8875–8883, http://dx.doi.org/10.1074/jbc.M110.187815, [Epub 2011 Jan 19].